Chem Soc Rev

Synthetic Applications of Hydride Abstraction Reactions by Organic Oxidants

Journal:	*Chemical Society Reviews*
Manuscript ID	CS-SYN-12-2021-001169.R2
Article Type:	Review Article
Date Submitted by the Author:	09-Jun-2022
Complete List of Authors:	Miller, Jenna; University of Pittsburgh Dietrich School of Arts and Sciences, Department of Chemistry Lawrence, Jean-Marc I. A.; University of Pittsburgh Dietrich School of Arts and Sciences, Department of Chemistry Rodriguez del Rey, Freddy; University of Pittsburgh Dietrich School of Arts and Sciences, Department of Chemistry Floreancig, Paul; University of Pittsburgh Dietrich School of Arts and Sciences, Department of Chemistry

ARTICLE

Synthetic Applications of Hydride Abstraction Reactions by Organic Oxidants

Jenna L. Miller,[a] Jean-Marc I. A. Lawrence,[a] Freddy O. Rodriguez del Rey[a] and Paul E. Floreancig*[a]

Received 00th January 20xx,
Accepted 00th January 20xx

DOI: 10.1039/x0xx00000x

Carbon–hydrogen bond functionalizations provide an attractive method for streamlining organic synthesis, and many strategies have been developed for conducting these transformations. Hydride-abstracting reactions have emerged as extremely effective methods for oxidative bond-forming processes due to their mild reaction conditions and high chemoselectivity. This review will predominantly focus on the mechanism, reaction development, natural product synthesis applications, approaches to catalysis, and use in enantioselective processes for hydride abstractions by quinone, oxoammonium ion, and carbocation oxidants. These are the most commonly employed hydride-abstracting agents, but recent efforts illustrate the potential for weaker ketone and triaryl borane oxidants, which will be covered at the end of the review.

A Introduction

Employing carbon–hydrogen bond functionalization reactions is an advantageous strategy in complex molecule construction that aligns well with the objectives of the various synthetic economies.[1] Avoiding the interchange of functional groups enhances atom economy,[2] while minimizing the formation of activating groups improves step economy.[3] Coupling carbon–hydrogen bond activation with target-relevant bond formation provides a strategy-level transformation that maximizes redox economy.[4] A more subtle advantage of utilizing carbon–hydrogen bond functionalization processes is that the minimization of activating groups mitigates compatibility issues with many reagents and allows for greater flexibility in sequence design. These attributes have led to a great expansion in the development of new transformations based on carbon–hydrogen bond functionalization and their applications in synthesis, as evidenced by numerous recent reviews.[5-15]

The preponderance of methods that are described in these reviews involve the use of transition metal catalysts for either direct or formal insertion into carbon–hydrogen bonds or radicals that abstract hydrogen atoms. The latter method frequently employs photoredox catalysis for generating reactive intermediates. A third class of reactions that is proving to be valuable in complex molecule synthesis proceeds via hydride abstraction to generate carbocations. All methods have unique attributes, with the hydride abstraction mechanism being distinguished by the availability and stability of the reagents, the lack of requirement for directing groups, the efficacy from the ground state, and a selectivity profile based on cation stability rather than homolytic bond dissociation energy.

This review will focus on the chemistry of hydride abstracting agents. These agents include quinones,[16] oxoammonium ions, and triarylmethyl (trityl) cations. Early examples of the use of these reagents will be provided followed by mechanistic discussions. Method development, including the applications in natural product syntheses, will be included. A discussion of the use of these agents as catalytic oxidants and as initiators of enantioselective bond formation will conclude the sections when applicable. The vast majority of the processes that have been reported are oxidations. Hydride abstraction reactions can also be redox neutral when coupled with a reductive step. While these transformations are not as widely developed, they show great promise in the design of useful bond-forming processes and will be included in the discussion.

B Quinone Oxidants

A Early Studies

Braude and co-workers conducted extensive studies on the use of quinones as dehydrogenating agents. Their hypothesis that these reactions proceed through cationic intermediates led them to explore dehydrogenation reactions that are accompanied by alkyl shifts.[17] This is illustrated (Scheme 1) by the reactions of 1,1-dimethyl tetralin (**1**) with 3,4,5,6-tetrachloro-1,2-benzoquinone (*o*-chloranil, **2**) or 2,3-dichloro-5,6-dicyano-1,4-benzoquinone (DDQ, **3**) to form 1,2-dimethylnaphthalene (**4**). The mechanism of this transformation was not discussed in detail, though a reasonable proposal involves the loss of the benzylic hydride to form a cation that loses a proton to form intermediate **5**. Abstraction of the allylic hydride of **5** generates a cation (**6**) that allows for a methyl group migration and proton loss to form **4**. Rigorous yield determinations were not reported in the manuscript, but DDQ proved to be significantly more reactive than *o*-chloranil.

[a] Department of Chemistry, University of Pittsburgh, Pittsburgh, Pennsylvania, USA 15260.

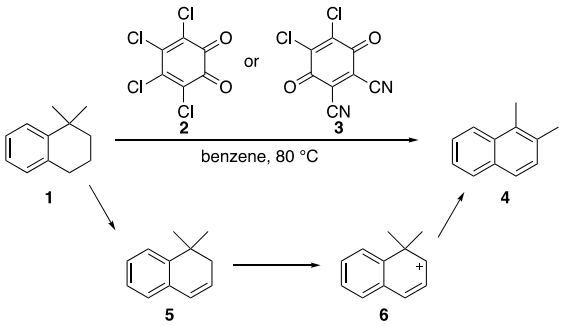

Scheme 1. Dehydrogenation with alkyl group migration.

Creighton and Jackman exploited the ability of DDQ to form cationic intermediates in the development of cyclodehydrogenation reactions (Scheme 2).[18] This process proceeds through the DDQ-mediated formation of benzylic carbocations followed by nucleophilic trapping. This is seen in the conversion of **7** to carbocationic intermediate **8** and, ultimately, to **9**. Notably the related conversion of **10** to **11** was much slower, indicating that cation formation is dependent on the number of appended stabilizing groups. The authors postulated that the dimeric side products (**12**) in the formation of **11** were the result of radical intermediates derived from **10**.

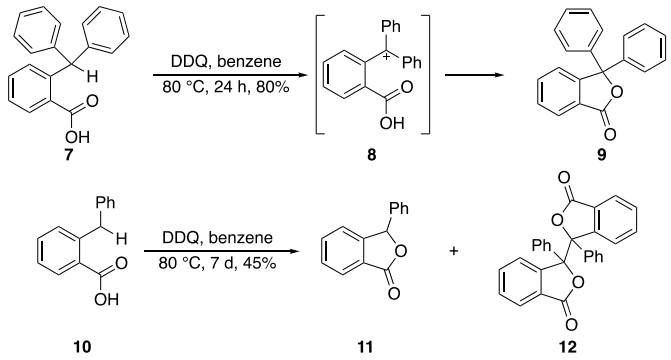

Scheme 2. Cyclodehydrogenation efficiency as a function of cation substituents.

Applications of DDQ in synthesis increased appreciably upon Horita's report that it can be used to cleave *para*-methoxybenzyl (PMB) ethers in the presence of water.[19] DDQ forms the stabilized benzylic cation from PMB ethers, as seen by the conversion of **13** to **14** (Scheme 3). Water adds to the oxocarbenium ion to form a hemiacetal intermediate that breaks down to form alcohol **15**. This process is selective for PMB ethers over benzyl ethers, which is consistent with the rate of oxidation correlating with the stability of the intermediate cation. 3,4-Dimethoxybenzyl (DMB) ethers are more reactive than PMB ethers, as seen by the conversion of **16** to **17**. This is not consistent with cation stability dictating the rates of these reactions, however, since methoxy groups at the *meta*-position slightly destabilize benzylic cations.[20] Additionally, differences in proximal functional groups and branching in proximity to the ether groups could be significant in determining hydride transfer rates.[21] These observations indicate that the mechanism of cleavage is likely more nuanced than previously considered. The complexity of the substrates in this study portended well for eventual applications in natural product synthesis.

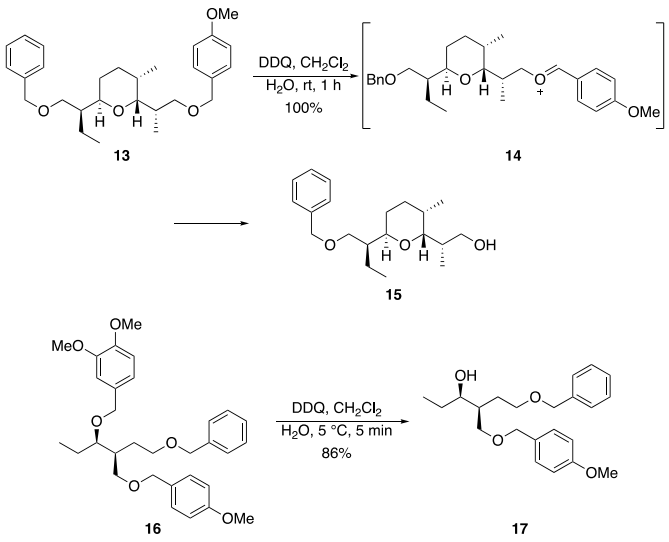

Scheme 3. Oxidative cleavage of electron rich benzylic ethers.

The examples to this point have contained arenes. Alkenes are also suitable substrates for DDQ-mediated oxidation. Yadav and co-workers reported[22] that allyl ethers can be cleaved under conditions that are similar to those that are used in PMB ether cleavage, though the process is considerably slower, and through an analogous mechanism. The selectivity in the cleavage of **18** to **19** (Scheme 4) can be attributed to the inductive effect at the anomeric allyloxy group diminishing the stability of a cationic intermediate. Vatèle showed[23] that prenyl ethers cleave faster than allyl ethers, as shown in the conversion of **20** to **21**. This is consistent with the ability of the methyl groups on the prenyl ether to stabilize the intermediate oxocarbenium ion. Aryl prenyl ethers do not cleave under these conditions (not shown), again demonstrating that inductive destabilization of the intermediate cation slows the oxidation.

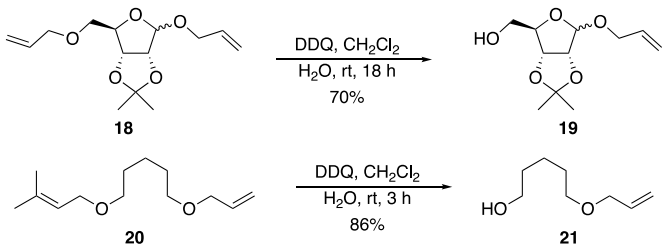

Scheme 4. Oxidative cleavage of allylic ethers.

B Mechanistic Investigations

The preliminary studies on DDQ-mediated oxidations clearly show that cationic intermediates are formed during the course of the reaction, indicating that the process is either a direct or formal hydride abstraction. Primary kinetic isotope effect studies show that carbon–hydrogen bond cleavage is the rate-

determining step, as seen in the dehydrogenation reaction of **22** to **24** via **23**[24] (Scheme 5) and in the oxidative cyclization of **25** to **27** via **26**.[25] Various mechanisms, however, can lead to these results.

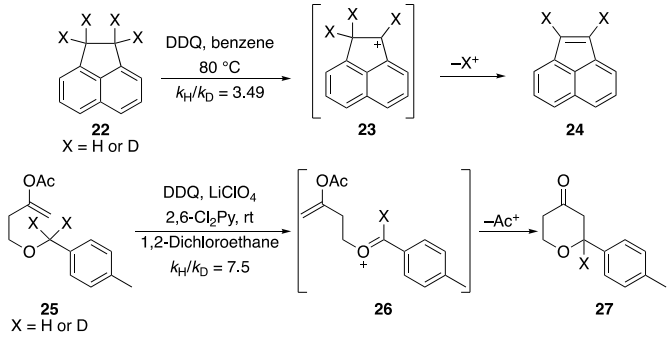

Scheme 5. Kinetic isotope effects studies for DDQ-mediated reactions.

Becker postulated[26] that DDQ-mediated oxidations proceed through the formation of a charge-transfer complex, based on the colour changes that arise upon mixing the reagents. The viability of these charge transfer complexes has been validated computationally.[27] Proton abstraction follows to generate radical intermediates. The radicals can react further, as seen (Scheme 6) in the conversion of **28** to radical **29** and then to **30**. Alternatively, cation formation can follow through a subsequent oxidation. This influential study was confined to phenolic substrates, however, opening the possibility that non-phenolic substrates could react through a different pathway. Single electron transfer between commonly encountered substrates and DDQ is prohibitively endergonic given the reduction potential of DDQ (0.5 V vs SCE)[28] and the oxidation potentials of common substrates (>1.4 V vs SCE).[29] The facile deprotonation of phenols would be expected to lower the oxidation potential and promote a single electron oxidation pathway. Single electron oxidation can be promoted by activating the quinone by hydrogen bonding. Turek and co-workers showed[30] that the capacity of *o*-chloranil (**2**) to act as an electron acceptor can be enhanced by several orders of magnitude upon complexation to hydrogen bond donor **31**. This promoted the oxidative cyclization of **32** to **33** in a process that the authors proposed to arise through an electron transfer pathway, although they conceded that a hydride transfer pathway was also possible.

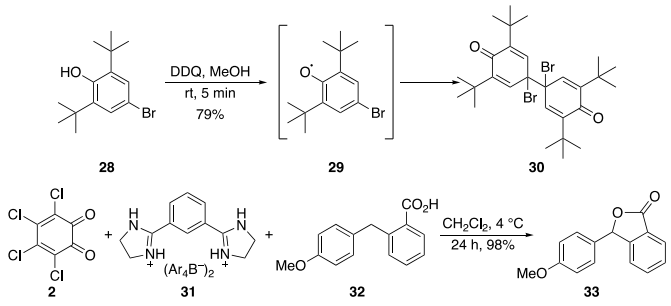

Scheme 6. Carbon–hydrogen bond functionalization through single electron transfer pathways.

Höfler and Rüchardt studied DDQ-mediated dehydrogenation reactions[31] and concluded that a hydrogen atom abstraction pathway was operative. This was based on their observation that, in the DDQ-mediated oxidation of **34**, the addition of nitrosobenzene (**35**) as a radical trap produced the expected signals of **36** in the epr spectrum (Scheme 7). The presence of this intermediate does not preclude alternate concurrent pathways, and the authors further proposed that hydrogen atom or hydride abstraction could be possible based on the substrate and solvent. This conclusion was supported by computations from Chan and Radom,[32] who showed that gas phase reactions between DDQ and hydrocarbon substrates predominantly proceeded through a hydrogen atom abstraction pathway, while substrates with a cation-stabilizing group in polar solvents undergo hydride abstraction.

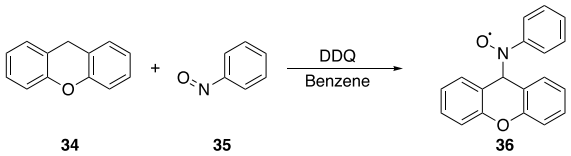

Scheme 7. Incorporation of a radical trap as a mechanistic probe.

Luca and co-workers validated the impact of incorporating a cation-stabilizing group through exposing benzylic amine **37** to DDQ and observing the rapid formation of iminium ion **38** (Scheme 8).[33] An accompanying computational study showed a mechanism that initially proceeds through the formation of a charge transfer complex followed by hydride transfer to the oxygen of DDQ to form phenolate **39**. A computational study by Guo and co-workers[34] and another by Yamabe[35] concurred with the conclusion that hydride transfer occurs on the oxygen of DDQ from hydrocarbon donors. However other donors such as tin hydrides can react through hydride transfer to a cyano-substituted carbon. The Guo study also described an experimental approach to determining the kinetics of hydride transfer from a wide range of donors.

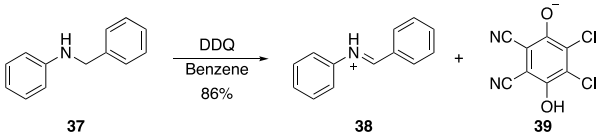

Scheme 8. Hydride transfer to form a stabilized cation.

Morales-Rivera and co-workers conducted a thorough computational study of the DDQ-mediated oxidation of benzylic, allylic, and vinylic ethers to form oxocarbenium ion intermediates (Scheme 9).[36] This study explored the energetics of the single electron, hydrogen atom, and hydride transfer pathways. The hydride transfer pathways to oxygen and carbon were compared. This study showed that the single electron and hydrogen atom transfer pathways for these substrates are prohibitively exergonic and cannot be considered as viable mechanisms for the C–H cleavage reaction. Hydride attacks at

oxygen and carbon show remarkably similar transition state free energies, though oxygen attack is significantly favoured thermodynamically due to the direct formation of an aromatic product.

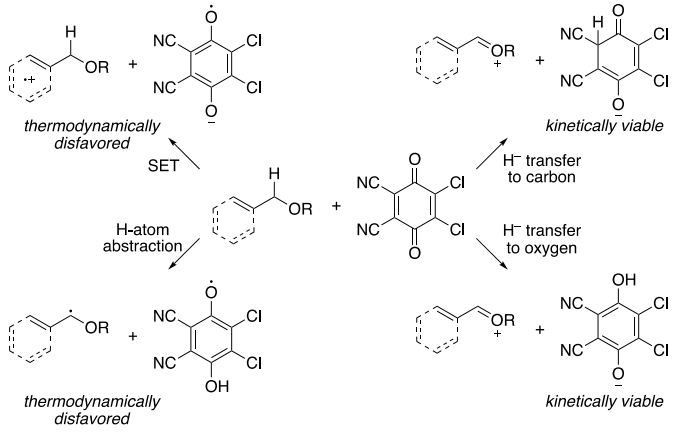

Scheme 9. Computational comparison of pathways for C–H cleavage.

Hydride abstractions from vinylic and allylic ethers proceed through transition states that have very different energies despite forming the same products (Scheme 10). The calculated transition state free energy for the oxidation of **40** to form oxocarbenium ion **41** is 15.6 kcal/mol while the corresponding value for the conversion of **42** to **41** is 20.8 kcal/mol despite the reaction of **42** being more exothermic. An analysis of the transition state structures showed that significantly more charge transfer occurs in the reaction of **40** compared to **42**. The oxidation potential of **40** is substantially lower than **42** by virtue of the oxygen lone pair donation into the alkene π-orbital,[37] and indicates that oxidation potential, in addition to the stability of the intermediate carbocation (as determined by the hydride dissociation energy), is important in dictating the kinetics of these reactions. The importance of charge transfer can be seen in the transition state geometry, illustrated by **43**, in which DDQ stacks on the π-system of the substrate.

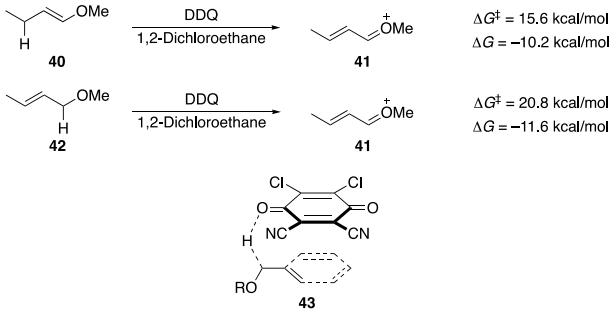

Scheme 10. Dependence of oxidation potential on transition state free energy, and the transition state geometry that maximizes the contribution of charge transfer stabilization.

Numerous insights arise from the analysis of these results. The high reactivity of 3,4-dimethoxybenzyl ethers in comparison to PMB ethers arises from the *meta*-methoxy group's lowering of the substrate oxidation potential, rather than influencing the stability of the cationic intermediate. This is also consistent with the significantly enhanced reactivity of enamides with DDQ relative to allylic amides.[38] Transition state free energies for DDQ-mediated hydride abstractions can be predicted by the empirically derived linear free energy relationship shown[39] in equation 1, where HDE is the hydride dissociation energy, and $E^0_{1/2}$ is the oxidation potential of the substrate.

$$\Delta G^{\ddagger}_{\text{predicted}} = 0.485\Delta G_{\text{HDE}} + 4.73E^0_{1/2} - 27.7 \qquad (1)$$

This equation does not predict the impact of steric effects on the transition state free energy. Hubig and co-workers reported that steric barriers can inhibit the formation of charge transfer complexes between arenes and quinones,[40] and Liu showed that incorporating a bulky trialkylsilyl group on the alkene of an allylic ether slows the oxidation significantly.[41] The impact of steric effects on oxidation rate was established in an experimental and computational study by Miller, Zhou, and co-workers.[42]

These studies provide a clear picture of the mechanism for carbon–hydrogen bond cleavage by DDQ. While the reactions of substrates that do not yield heteroatom-stabilized carbocations potentially proceed through competitive hydrogen atom abstraction and hydride abstraction mechanisms, the oxidations of substrates that form heteroatom-stabilized carbocations clearly proceed through a hydride abstraction mechanism. This leads to cation stability being a critical component in the transition state free energy. The stacked orientation of the substrate π-system with DDQ in the transition state allows for charge transfer to be an important factor in the barrier of the reactions, also making substrate oxidation potential an important contributor to reaction kinetics. This transition state geometry leads to a significant sensitivity to steric effects on reaction rates.

C Applications to Bond Forming Reactions

1 Bimolecular reactions

The use of DDQ-mediated hydride abstraction in productive bond-forming processes is complicated by the need to conduct the reactions under rigorously anhydrous conditions and to employ substrates and nucleophiles that react with high selectivity under oxidative conditions. Hayashi and Mukaiyama reported[43] a significant advance toward this objective in 1987 in which cinnamyl ethers act as precursors to electrophiles for relatively weak nucleophiles. This is illustrated (Scheme 11) by the reaction of ether **44** with DDQ and TMSCN in the presence of $LiClO_4$ to form cyanohydrin ether **45** in excellent yield. This transformation results from hydride abstraction to form an oxocarbenium ion intermediate, and $LiClO_4$ serves as an ion exchange reagent to form a more reactive ion pair. Allylstannanes and enolsilanes can also act as nucleophiles though, in contrast with the reaction with TMSCN, the oxidation must proceed to completion prior to nucleophilic addition

(cation pool approach[44]) since these reagents react competitively with DDQ. Remarkably, this process was not significantly exploited further until Ying and co-workers expanded the scope of the hydride donors to include benzylic ethers.[45] These substrates required electron-donating groups on the arene, as seen in the aldol-like conversion of ether **46** to **47**. $LiClO_4$ again was shown to be useful for the process, and molecular sieves were added to ensure anhydrous conditions. The oxidation was run to completion prior to the addition of the nucleophile in accord with the previous study's observation of functional group incompatibility between enolsilanes and DDQ.

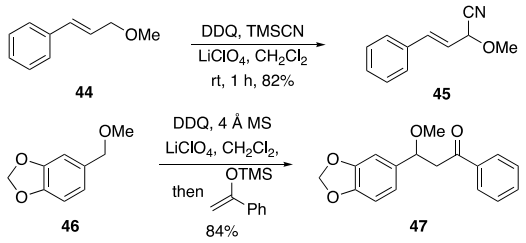

Scheme 11. Initial examples of DDQ-mediated oxidative carbon–carbon bond formation.

Zhang and Li explored the possibility of utilizing DDQ-mediated hydride abstraction in cross-dehydrogenative-coupling (CDC)[46] reactions. These processes deliver bond formation with a formal loss of H_2 and alleviate the need for pre-forming the nucleophile. This is illustrated through the coupling of isochroman (**48**) with acetophenone (**49**) in the presence of DDQ to form **50** in good yield (Scheme 12).[47] These reactions are conducted in the absence of solvent at elevated temperature with an excess of the nucleophile. The authors propose that the DDQ-derived phenolate acts as a base to generate an enolate, though the weak basicity of this species is unlikely to generate the nucleophile. The enol form of the ketone is most likely the relevant nucleophile. The same authors showed[48] that significantly more acidic nucleophiles react under much milder conditions in the presence of catalytic amounts of $InCl_3$ and $Cu(OTf)_2$, as shown in the conversion of **48** with **51** to form **52** at room temperature. Although the role of the additives is not clear, they could possibly enhance the acidity of the nucleophile to promote deprotonation, or they could activate DDQ to enhance its hydride affinity. Both reports indicate that acyclic benzyl ethers can be used as substrates, but their reactions are significantly less efficient.

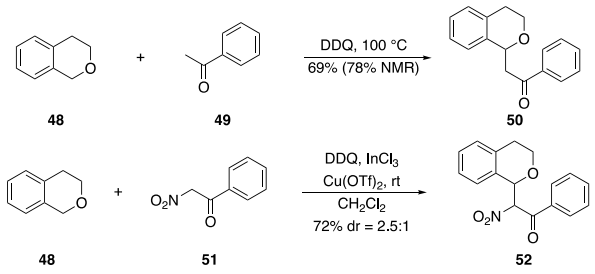

Scheme 12. Initial developments in DDQ-mediated CDC reactions.

The isochroman motif has proved to be a very valuable test unit for developing new oxidative bond-forming processes. Park and co-workers showed that isochroman can engage in a reaction that appears to be a Friedel-Crafts alkylation in the presence of an electro-rich arene, DDQ, and $CuCl_2$ (Scheme 13),[49] as seen in the coupling of **48** and **53** to form **54**. TEMPO suppresses this reaction, indicating that it proceeds through a radical pathway and that it is not a simple oxidative Friedel-Crafts process. The authors propose a mechanism that proceeds through the addition of an aryl radical to an oxocarbenium ion. Cao and co-workers showed that this type of reaction can be done to functionalize methine groups in the absence of $CuCl_2$.[50] This work employed electron-rich heterocycles in the generation of quaternary centres, as seen in the oxidative union of **54** and **55** to form **56**. The same group showed that potassium alkynyl trifluoroborates can add to similar oxocarbenium ions.[51] This reaction required the addition of $LiBF_4$, which the authors proposed to create a more reactive ion pair intermediate. This transformation is seen in the coupling of **57** and **58** to form **59**.

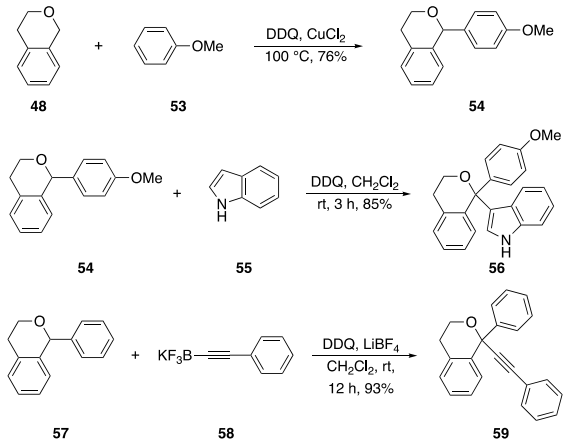

Scheme 13. Further functionalization of isochroman and its derivatives.

Clausen demonstrated the impact of generating aromatic cations on increasing reaction rates.[52] Isochromene **60** reacts with DDQ to generate aromatic cation **61** within 10 min at –30 °C (Scheme 14). This contrasts the elevated temperature and prolonged reaction time that was employed in the oxidation of **48** in the absence of Lewis acidic additives (Scheme 12). The $LiClO_4$ that is added for this process is used to create a more reactive ion pair rather than enhance the oxidation rate. Adding allyl tributyltin delivered **62** in good yield. This method can also be utilized in the oxidation of chromenes, even when an electron-withdrawing group is appended. Cyano-substituted chromene **63** can be oxidized at elevated temperatures and, upon cooling, reacts smoothly with allyl trimethylsilane to form **64**.

Benzo-fused nitrogen-containing heterocycles are also excellent substrates for DDQ-mediated functionalization, with *N*-aryl tetrahydroisoquinolines being particularly common substrates. Tsang and Todd showed[53] that conducting a DDQ-mediated oxidation of **65** in $MeNO_2$ solvent resulted in the

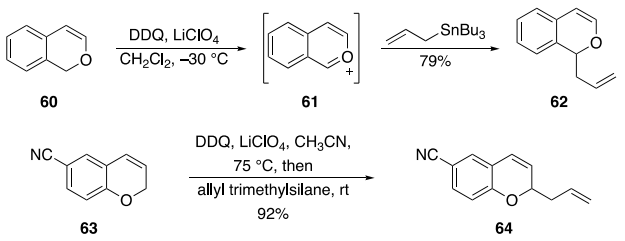

Scheme 14. Oxidatively-generated aromatic cations in bond-forming reactions.

formation of iminium ion **66** and then to alkylation product **67** (Scheme 15). Notably, the ion pair of **66** and the DDQ-derived phenolate could be isolated and characterized.[54] The stability of the intermediate adduct allows for other nucleophiles to be utilized in the process, as evidenced by the Friedel-Crafts alkylation under ball milling conditions to form **68**[55] and the oxidative phosphonate formation to yield **69**.[56] Ravindran and co-workers showed the utility of generating aromatic intermediates from nitrogen-containing heterocycles.[57] Exposing **70** to DDQ provided pyridinium ion **71** within 5 min. Base-mediated hydrolytic rearrangement resulted in the formation of **72**.

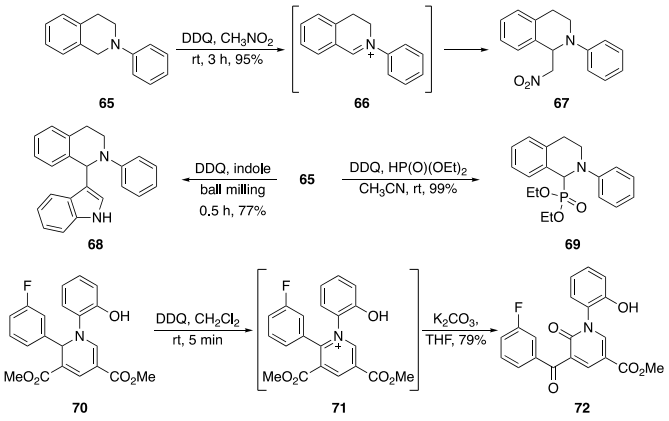

Scheme 15. Oxidative functionalization of *N*-aryl tetrahydroquinolines.

Substrates that do not contain a cation-stabilizing heteroatom can also be used in oxidative bond-forming reactions if they can provide an intermediate cation that is sufficiently stabilized through resonance. Diarylmethane and diaryl propene compounds are particularly useful in these transformations. Correia and Li developed a cross-dehydrogenative-coupling approach to alkynylate diphenylmethane (**73**) with phenylacetylene (**74**).[58] The authors proposed the *in situ* formation of a copper acetylide that acts as a nucleophile to react with the intermediate carbocation and form **75** (Scheme 16). 1,3-Diphenyl-1-propene (**76**) undergoes oxidation under much milder conditions than **73**. Cheng and Bao showed that **76** reacts with DDQ and diketone **77** (presumably as its enol tautomer) within 1 h at rt to form **78** in good yield.[59] Interestingly, when electron-donating groups are appended to the arenes the reactions are somewhat slower, indicating that the rate determining step in those transformations could be nucleophilic addition rather than hydride abstraction. Other nucleophiles can be used to add into diarylpropene-derived cations, including indole,[60] phosphites,[61] and enaminones.[62]

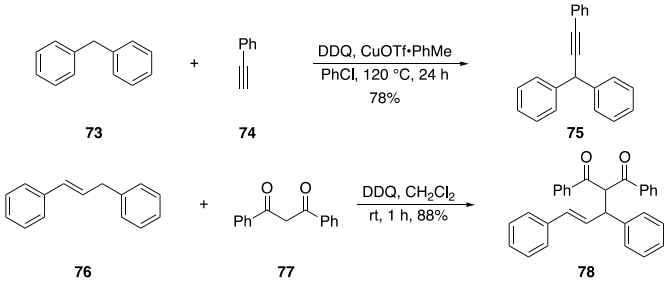

Scheme 16. Oxidative hydrocarbon functionalization.

Cheng and co-workers expanded the diarylpropene chemistry in the development of processes that employ consecutive oxidations.[63] This is illustrated (Scheme 17) by the coupling of **76** with enamino ester **79**. Mechanistic studies showed that this process initially delivers **80**, the product of carbon–carbon bond formation, followed by a second oxidation to promote carbon nitrogen bond formation (preceded by alkene isomerization) and finally a terminal oxidation to form **81** through aromatization. This showed that both termini of the propene core can be functionalized, but variations in the nucleophile structure can deliver products in which the same carbon is functionalized twice.[64] This is seen in the coupling of **76** with amide **82** to yield **83**.

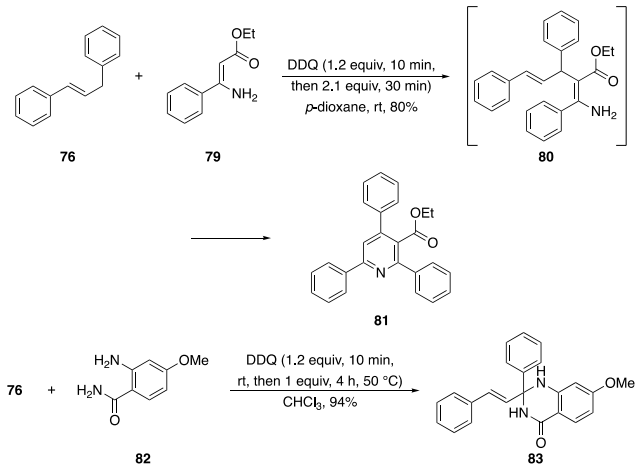

Scheme 17. Annulation through consecutive oxidations.

2 Intramolecular reactions with carbon nucleophiles

The reactions shown in Scheme 17 confirmed that oxidative cyclization reactions are possible when the nucleophilic group is compatible with DDQ. Prior studies showed that, among common nucleophiles for carbon–carbon bond formation through reactions with stabilized carbocations, allylsilanes are compatible with DDQ while enolsilanes are not.[45] Tu and Liu reported that enol acetates can act as enolsilane surrogates that are stable to DDQ, yet react efficiently with oxidatively generated oxocarbenium ions (Scheme 18).[65] This is shown by the oxidation of PMB ether **84** to generate oxocarbenium ion **85**, which orients in a chair-type transition state to form **86** as a single stereoisomer. The rates of the reactions correlate with the stabilities of the intermediate cations and the substrate oxidation potentials, in accord with previously discussed computational studies.[36] Allylic ethers are also suitable substrates for this protocol as shown by the conversion of **87** to **88**. This transformation was somewhat slower than many in the report due to the inductive destabilization of the intermediate carbocation by the acetoxy groups. The 2,6-dichloropyridine is not necessary as a base in these reactions but improves yields through scavenging the acylium ions that form during the nucleophilic addition step.

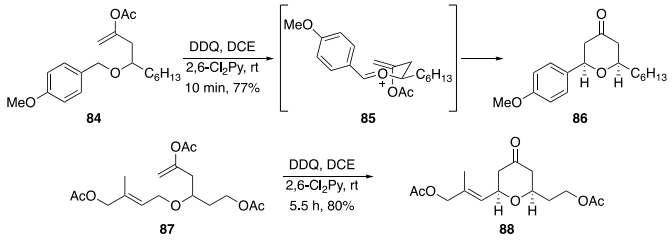

Scheme 18. Stereocontrolled oxidative annulation with carbon–carbon bond formation.

Yu and co-workers expanded upon these results to show that terminal alkenes can act as effective nucleophiles toward oxidatively generated oxocarbenium ions when the reactions are conducted in the presence of $SnBr_4$ (Scheme 19).[66] Ether **89** reacts under these conditions to form intermediate species **90**. The role of $SnBr_4$ in this process is not discussed at length in this report. One possibility is that the Lewis acid can activate DDQ to enhance its reactivity as a hydride-abstracting agent. The resulting complex with the DDQ-derived phenolate would create a more reactive ion pair for the weaker nucleophile, then the complex can act as a bromide source in the formation of **91**. The stereochemical outcome of the reaction is consistent with established transition states for Prins-type cyclizations, as described in several reviews.[67-69] Ghosh and Xu reported that allylsilanes act as nucleophiles when PPTs is employed as an additive.[70] The conversion of cinnamate ether **92** to **93** illustrates this process. The mild Brønsted acid proved to be more effective than Lewis acids in promoting this process.

Subba Reddy and co-workers showed that DDQ-mediated oxocarbenium ion formation can be used to initiate cascade reactions that form two rings (Scheme 20).[71] Diol monoether **94**

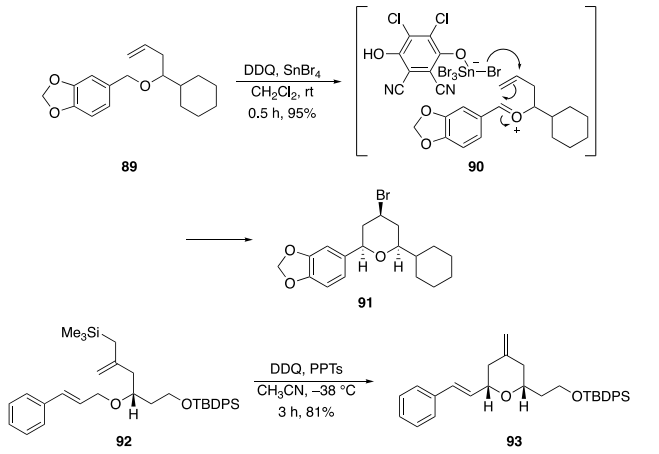

Scheme 19. Additional nucleophiles in oxidative cyclization reactions.

reacts with DDQ in the presence of $In(OTf)_3$ to form oxocarbenium ion **95**. Cyclization through the conformation shown in **95** provides bicycle **96** in good yield as a single diastereomer. The transition state model predicts that the stereochemical outcome of this process can be altered by changing the geometry of the alkene. This is validated by the oxidation of **97** to form **98**.

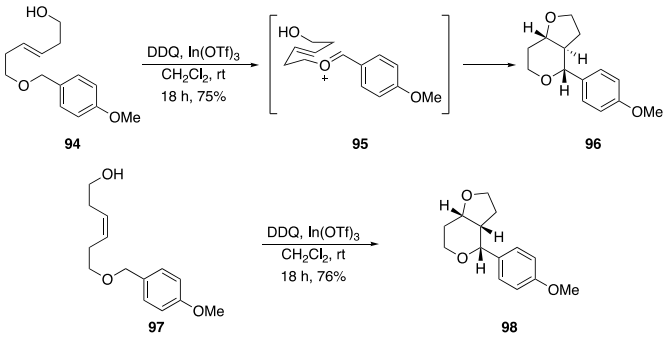

Scheme 20. Oxidative cascade cyclizations.

The ability to generate oxocarbenium ions under mild oxidative conditions allows for explorations on their conformational preferences and stabilities. Liu reported that employing propargylic ethers as substrates, rather than allylic or benzylic ethers, resulted in significantly slower cyclization reactions (Scheme 21).[72] This is seen in the oxidation of **99**, which formed a mixture of oxocarbenium ions **100*E*** and **100*Z***. Ring closure produced tetrahydropyranones **101** and **102** in an approximately 1.6:1 ratio. Oxocarbenium ions generally show a strong preference for the *E*-geometry due to the avoidance of steric effects,[73] but the linear geometry of the alkynyl group appears to mitigate the steric destabilization of the *Z*-isomer.

The same authors explored whether predictable stereochemical outcomes for these reactions could be achieved for products that contain tertiary ethers. A series of secondary allylic and benzylic ethers were oxidized by DDQ to determine whether fully substituted oxocarbenium ions could have a geometrical preference (Scheme 22).[74] Several substrates

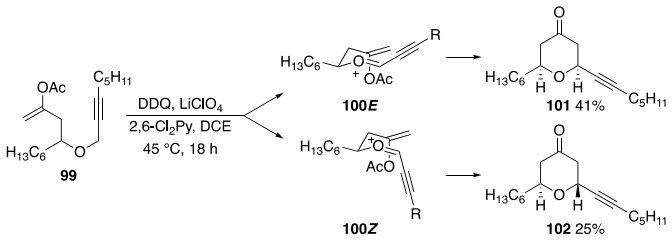

Scheme 21. Stereochemical outcome with alkynyl-substituted oxocarbenium ions.

proceeded through oxidative cyclization reactions with high degrees of stereocontrol. Ether **103** underwent oxidative cyclization to form oxocarbenium ion **104** and then **105** as a single stereoisomer in good yield. This study also investigated the possibility for a tertiary ether to influence the stereochemical outcome of an addition into an oxocarbenium ion. The conversion of **106** to **107** showed that stereocontrol relative to a fully substituted centre can be quite high. Predictive models that explain these results are illustrated by **108** and **109**. The fully substituted oxocarbenium ion can be explained by a steric model, whereby the smaller substituent prefers the *cis*-orientation relative to the other chain. This model accurately predicts other intramolecular additions into oxocarbenium ions to form tertiary ether products.[75,76] The model for the influence of a tertiary ether is proposed to arise from an electrostatic attraction between a π-system and the partially positively charged hydrogen on the oxocarbenium ion.

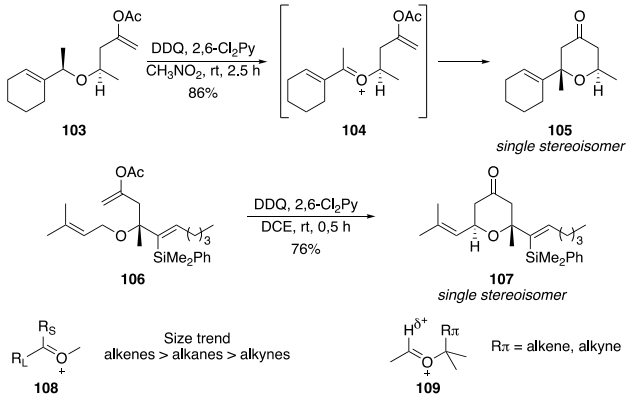

Scheme 22. Stereoselective construction of tertiary ethers.

Electrostatic effects can also be invoked to explain the rare formation of 2,6-*trans*-dihydropyrans in Prins-type cyclizations.[77] Han coupled the results from the studies in Schemes 21 and 22 with the use of a tethering strategy to design systems that preferentially form 2,6-*trans*-tetrahydropyrans.[78] This is illustrated (Scheme 23) through the oxidative conversion of **110** to macrocyclic oxocarbenium ion **111**, in which the alkynyl group exists in an axial orientation due to the geometric constraints imposed by the tether and the electrostatic attraction between the π-bonds with the hydrogen on the oxocarbenium ion. Closure to form product **112** showed that the common stereochemical outcome for Prins-type cyclizations can be reversed through rational design. This is also true for propargylic ether substrates, though the efficiencies of the cyclizations are not as high. Oxidizing macrocyclic ether **113** produced (*Z*)-oxocarbenium ion **114** as a precursor to bridged bicycle **115**. This result indicates that the modest preference for alkynyl oxocarbenium ions to exist in an *E*-configuration can readily be overcome by the geometrical constraints of the tether.

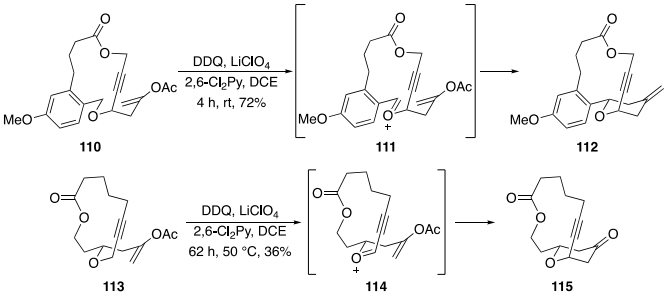

Scheme 23. Dictating stereochemical outcomes by tethering.

As seen in the oxidations of *N*-aryl tetrahydroisoquinolines, highly stabilized iminium ions can be formed from amine oxidations. Acyliminium ions could, in principle, be formed through the oxidation of allylic amides or carbamates, though these species are generally inert toward DDQ.[38] Brizgys and co-worked showed[79] that alkenyl amides and carbamates, however, are excellent substrates for DDQ-mediated acyliminium ion formation. This arises from their lower oxidation potential in comparison to allylic amides. This has been utilized in stereoselective cyclization chemistry, as shown in Scheme 24. The mild conditions to form structurally unique acyliminium ions allowed for the examination of their transition states in intramolecular reactions. This is illustrated in the oxidation of vinyl lactam **116** to form acyliminium ion **117**, in which the *E*-geometry is preferred and the nucleophile aligns in an axial orientation due to an electrostatic interaction between the carbonyl oxygen and the developing positive charge on the allylsilane in the transition state. Ultimately this produces bicycle **118** as a single stereoisomer. This process was very efficient and proceeded in just 3 min at rt. Sulfonyliminium ions are also accessible through alkenyl sulfonamide oxidation, as illustrated by the conversion of **119** to **120**. These reactions are slightly less efficient and stereoselective than the reactions with vinyl amides and carbamates but still deliver useful product quantities. The relative stereocontrol of the amides and carbamates is opposite to that of sufonamides due to the electrostatic attraction between the amide carbonyl and the developing positive charge in the nucleophile not being present in the sulfonamides.

Allylic sulfonamides can be converted to sulfonyliminium ions when oxidative C–H cleavage is accompanied by aromatization. Kar and co-workers demonstrated this (Scheme 25) in the conversion of indolene **121** to cationic indole derivative **122**.[80] An intramolecular Friedel-Crafts alkylation

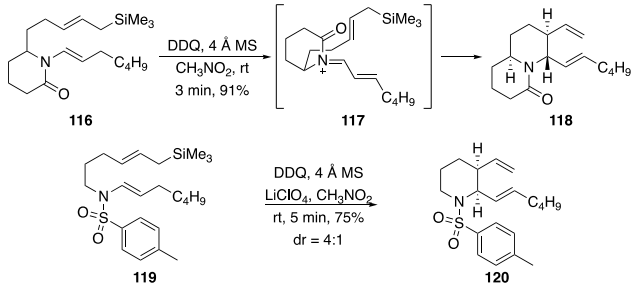

Scheme 24. Cyclizations through oxidatively-generated acyliminium and sulfonyliminium ions.

reaction provided fluorene-substituted indole **123**. Notably the isomeric substrate in which the indole nucleus is intact reacted far less efficiently, demonstrating the importance of starting material energy on oxidation rates. The same group showed that the incorporation of aniline nucleophiles into these reactions can be utilized to fuse quinoline units to indoles, as seen in the oxidation of **124** to **125**, through sequential oxidations.[81]

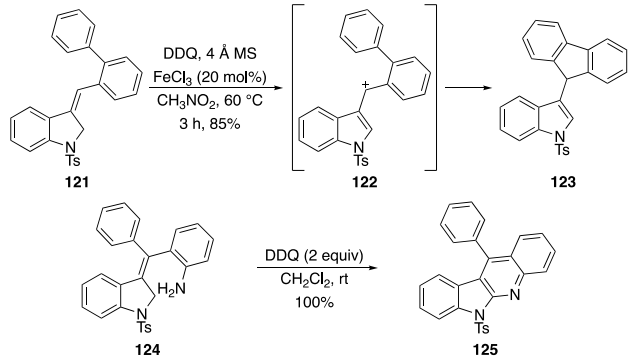

Scheme 25. Aromatization-assisted oxidation of allylic sulfoxides.

Cross-dehydrogenative-coupling reactions are possible between oxidatively generated iminium ions and properly selected nucleophiles. This was demonstrated by Grenning and co-workers in their efforts toward diversifying complex molecular scaffolds (Scheme 26).[82] Exposing amine **126** to DDQ nearly instantaneously produced the expected iminium ion. Numerous nucleophiles couple with this species, as illustrated by the addition of indole to form **127**. Jung and Min demonstrated a dehydrogenative cyclization[83] by exposing tetrahydroisoquinoline **128** to DDQ in the presence of $LiClO_4$ formed iminium ion **129**, which cyclized to form **130** with excellent stereocontrol, presumably via an enol addition through a chair transition state. Although not a cross-dehydrogenative process, Jo and co-workers designed a substrate that allowed for the formation of bridged bicyclic amines.[84] This is illustrated through the DDQ-mediated conversion of **131** to **132**. The rapid rate for this reaction reflects the exceptional ability of nitrogen to stabilize adjacent cations. The authors did not discuss the origin of the oxidation regioselectivity, though this presumably arises from the low degree of overlap between the methine C–H bond and the nitrogen lone pair as a result of a conformation in which allylic 1,2-strain is minimized.

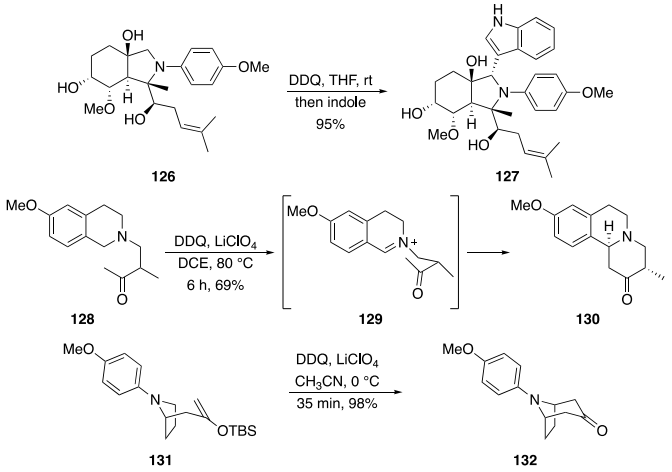

Scheme 26. Dehydrogenative carbon–carbon bond formation through oxidatively generated iminium ions.

Cui demonstrated that thiocarbenium ions are accessible through the oxidation of allylic or vinyl sulfides (Scheme 27) and undergo efficient cyclization reactions.[85] The products of these reactions show competitive reactivity with allylic sulfide starting materials, so yields with the more reactive vinyl sulfide substrates are superior. These reactions can proceed with high stereocontrol, as seen in the conversion of **133** to **134** and then to **135**, indicating that thiocarbenium ions also have a strong preference for the *E*-geometry. The longer carbon–sulfur bond relative to a carbon–oxygen bond allows for 5-*endo*-cyclizations to be viable. This is seen in the highly stereoselective conversion of **136** to tetrahydrothiophene **138** via (*E*)-thiocarbenium ion **137**.

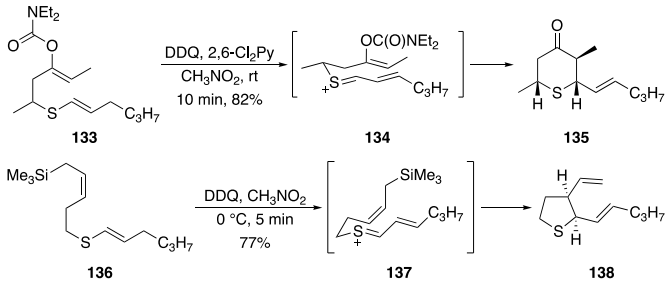

Scheme 27. Oxidative approach to sulfur-containing heterocycles.

Wang and co-workers showed that ketene dithioacetals can add to oxidatively generated cations to form substrates for a subsequent annulation reaction (Scheme 28).[86] This is shown through the addition of ketene dithioacetal **139** to diarylmethane **140** in the presence of DDQ. Loss of a proton

from the intermediate formed the highly oxidizable structure **141**. A second equivalent of DDQ abstracts the benzylic hydride to form cation **142**, which proceeds through an intramolecular Friedel-Crafts cyclization to yield **143**. This is an excellent illustration of a double cross-dehydrogenative annulation reaction.

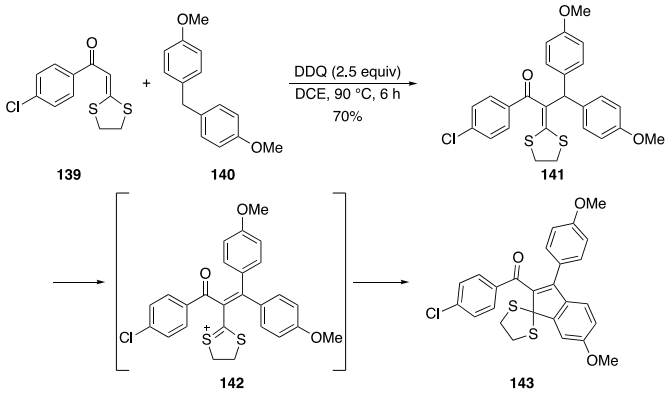

Scheme 28. Oxidative annulation through a sulfur-stabilized carbocation.

3 Intramolecular reactions with heteroatom nucleophiles

Heterocycles can also be prepared through the addition of heteroatom nucleophiles to oxidatively generated carbocations, provided that the nucleophile is stable towards the oxidant. Hubert and co-workers provided an excellent example of this in their studies on sesterterpenoid spiroketals (Scheme 29).[87] This process employed the conversion of dihydropyran **144** to oxocarbenium ion **145**. The pendent alcohol nucleophile coupled with this electrophile to form spiroketal **146** with complete stereocontrol. The origin of the selectivity for cleaving the carbon–hydrogen bond of one allylic ether in the presence of another allylic ether and an allylic alcohol illustrates the unique selectivity that can be observed with DDQ, even when two similarly substituted ethers are present in the same molecule. Peh reported a similar transformation in which the exceptional chemoselectivity of DDQ was exploited for the design of a telescoped transformation that merged fragment coupling and spirocyclization.[88] Allylsilane **147** adds to dihydropyran **148** in the presence of TMSOTf to form **149** through a Ferrier reaction. Adding a minimal amount of aqueous $NaHCO_3$ to cleave the silyl ether followed by DDQ provided **150** in good yield and with high stereocontrol for the convergent one-pot spiroketal synthesis.

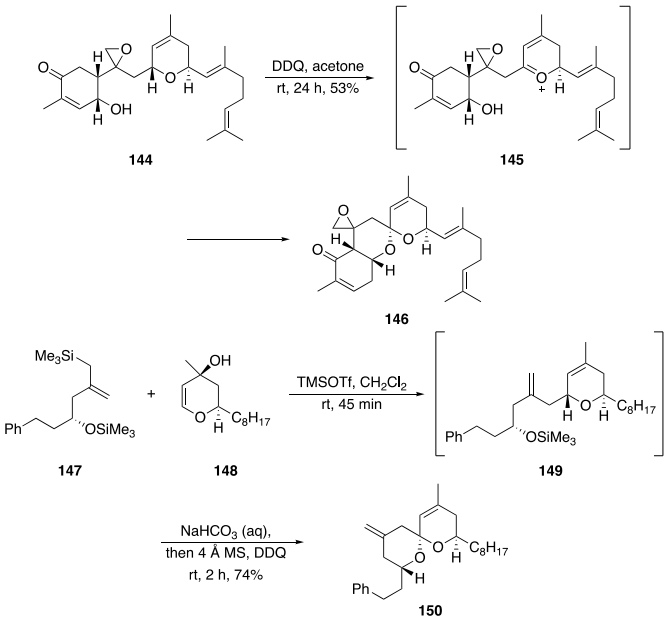

Scheme 29. Oxidative spiroketal formation.

Heteroatom-rich heterocycles can be prepared through the oxidation of oxime derivatives (Scheme 30). Lemercier and Pierce showed that the oxidation of thiohydroxamic acid derivatives can be converted to 1,4,2-oxathiazoles, as shown by the conversion of **151** to **152**.[89] The high reaction temperature most likely reflects the diminished capacity of the thiohydroxamate group relative to a sulfide to stabilize the intermediate carbocation. Similarly, amidoximes can be converted to 1,2,4-oxadiazoles as shown in the reaction of **153** to **154**.[90] Trivalent nitrogen allows these processes to continue to aromatize.

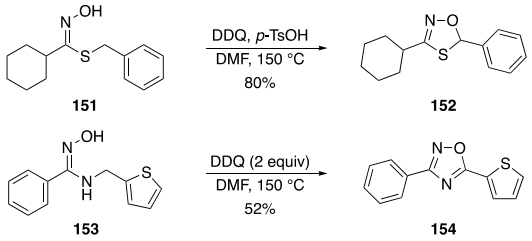

Scheme 30. Oxidative route to heteroatom-rich heterocycles.

Oxidative cyclizations can be conducted on substrates that lack a heteroatom to stabilize the intermediate carbocations, provided that sufficient stabilization is provided through conjugation. Yu and co-workers demonstrated this in their oxidative approach to dihydropyrans (Scheme 31).[91] These reactions proceed through the oxidation of aryl-substituted alkenes to form cinnamyl cations. This is illustrated by the oxidation of **155** to form **156**, in which the cisoid allylic cation enforces the boat-like conformation for the cyclization transition state and the substituent on the stereocenter avoids steric interactions. This leads to the formation of 2,6-*trans*-disubstituted dihydropyran **157**. The stereocontrol in this example is quite high, though smaller substituents lead to diminished diastereomeric ratios. Reaction efficiency is maximized in systems in which the arene contains an electron-donating group.

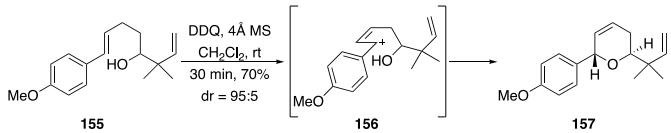

Scheme 31. Cyclization through allylic cation formation.

Nitrogen nucleophiles are particularly prone to undergo oxidation. However Wen and co-workers demonstrated that azido groups are stable toward DDQ, even at elevated temperatures. This allows for the formation of nitrogen-containing heterocycles, as shown in Scheme 32.[92] Oxidizing azide **158** with DDQ in the presence of trifluoroacetic acid (TFA) cleaves the benzylic C–H bond, leading to the azido group adding to form intermediate **159**. Hydride migration to nitrogen releases N_2, and proton loss forms cyclic imine **160**. Extension to the formation of six-membered rings was unsuccessful due to preferential alkyl group migration to form ring contracted products. This is illustrated by the oxidation of **161** to form cyclized product **162**. Alkyl group migration and reduction of the resulting iminium ion with $Na(AcO)_3BH$ generates benzylic pyrrolidine **163**. This sequence of oxidation and reduction leads to a formal insertion of nitrogen into a benzylic carbon–carbon bond. These results indicate that alkyl group migration is favored over hydride migration unless it leads to a strained ring.

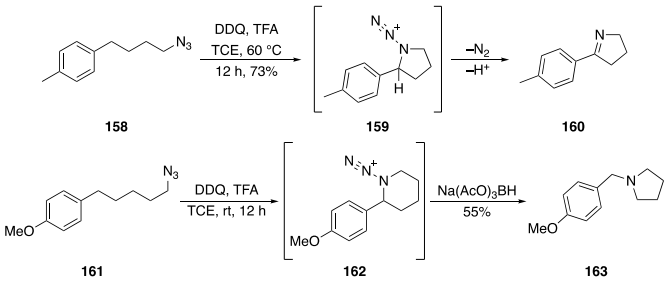

Scheme 32. Azides as nitrogen nucleophiles in oxidative cyclizations.

4 Oxidative bond reorganization reactions

Oxidative carbon–hydrogen bond cleavage can introduce functional groups or reactive intermediates into molecules that create the possibility for cycloaddition or rearrangement reactions. This is quite useful for rapid increases in molecular complexity.

Numerous examples of dehydrogenative Diels-Alder reactions are known, though these processes are complicated by the potency of DDQ as a dienophile. This was seen in the work of Qi and co-workers as they merged dehydrogenation with silver nanoparticle-catalyzed cycloaddition (Scheme 33).[93] Exposing prenylated chalcone **164** to DDQ and silica-supported silver nanoparticles produced diene **165**. While cycloaddition with DDQ occurred at lower temperatures, conducting the reactions at higher temperatures resulted in a retro Diels-Alder reaction followed by the desired cycloaddition to form **166**. Additional studies showed that the silver nanoparticles catalyze both the Diels-Alder and the retro Diels-Alder reactions, as predicted by microscopic reversibility.

Zhou and co-workers employed dehydrogenative Diels-Alder reactions to fuse rings onto 2,3-dialkyindole units.[94] This is illustrated (Scheme 34) by the conversion of **167** and **168** to spirocycle **169**. The diastereocontrol in this reaction was good, but the relative stereochemistry in the major stereoisomer was

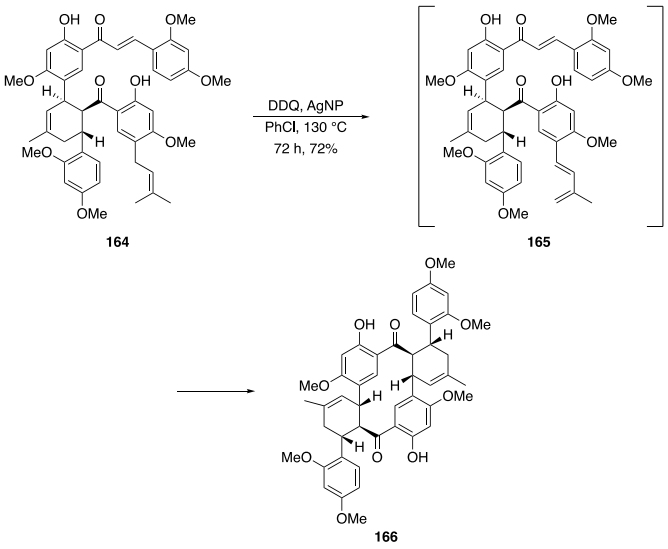

Scheme 33. DDQ-mediated dehydrogenative Diels-Alder reaction.

not reported. Reactions that do not form a quaternary center can react further to yield aromatized products, as seen in the conversion of **167** and *N*-phenylmaleimide (**170**) to carbazole **171**. The authors did not report on competitive cycloaddition of the intermediate dienes with DDQ, possibly because the dienophiles that were employed are also extremely reactive. Similarly, Manna and Antonchick reported[95] that *p*-cymene (**172**) can be oxidized in the presence of benzoquinone and 2 equiv DDQ to form **173** via the intermediate styrene. The reaction required acidic activation of benzoquinone by hydroquinone.

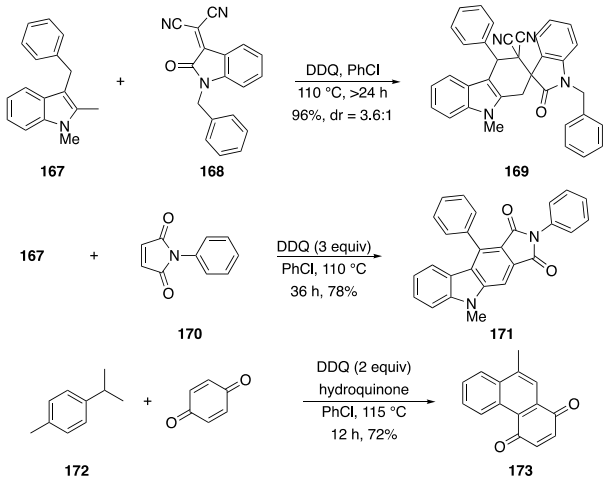

Scheme 34. Oxidative ring fusion onto arenes.

After observing that dehydrogenative diene-forming reactions lead to rapid cycloadditions with DDQ,[96] Xu and co-workers demonstrated that the initial adducts undergo retro Diels-Alder reactions to regenerate dienes that react with other dienophiles (Scheme 35).[97] Alkene **174** reacts with tetracyanoethylene (**175**) in the presence of DDQ to form

cycloadduct **176** at 115 °C. Lower temperatures generate **176** and DDQ-adduct **177**. The ability of **177** to undergo a retro Diels-Alder reaction followed by a different Diels-Alder reaction was demonstrated by heating it to 115 °C in the presence of **175** and obtaining a high yield of **176**. The same group showed that both components of a Diels-Alder reaction can be generated through dehydrogenation.[98] Alkene **174** undergoes dehydrogenation in accord with the previous reaction, while diketone **178** proceeds through a pathway that requires DDQ and Cu(I). Conducting these processes simultaneously results in the formation of **179** in high yield. Experiments in the presence of TEMPO suppressed the formation of **179**, suggesting that at least one of the two dehydrogenation reactions proceeds through a radical intermediate.

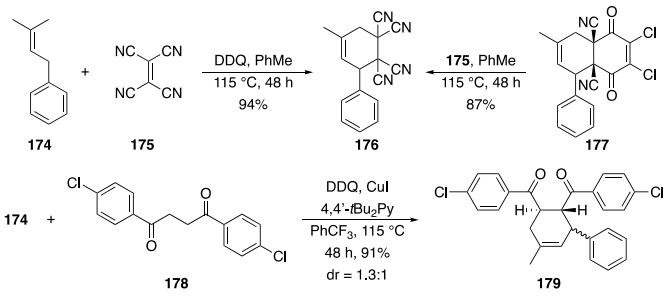

Scheme 35. Diels-Alder adducts from retro Diels-Alder reactions of DDQ adducts.

Two highly creative oxidative rearrangements are shown in Scheme 36. Fradette and co-workers demonstrated that oxidative carbocation formation can be utilized to initiate Nazarov cyclizations.[99] This is demonstrated through the conversion of 1,4-diene **180** to oxocarbenium ion **181**, in which the benzyl group acts as the equivalent of a Lewis acid in a classical Nazarov reaction. Conrotatory ring closure and regioselective proton loss led to the formation of **182** in good yield. Zhao and co-workers reported that ether oxidation can lead to a bond rearrangement through sequence of oxonia Cope and Prins reactions.[100] Exposing **183** to DDQ formed the expected benzylic oxocarbenium ion, which underwent a [3,3]-rearrangement to form **184**. Addition of the enolsilane to the oxocarbenium ion produced **185**. This transformation could also proceed through an initial Prins reaction followed by a pinacol reaction.

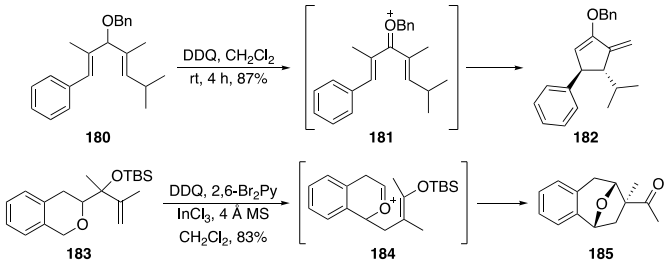

Scheme 36. Oxidative rearrangement reactions.

5 Applications to natural product synthesis

The diverse reactivity and functional group tolerance of DDQ have made it a common reagent for applications in the late stages of natural product syntheses. Many of these applications involve the release of protecting groups or aromatization reactions. Rather than focusing on these ubiquitous processes, this section will explore strategy-level reactions that increase molecular complexity and incorporate functional groups that are present in the target.

Xu and co-workers reported an early example of oxidative bond formation in natural product synthesis in their route to deoxyfrenolicin (Scheme 37).[101] This sequence proceeded through the oxidation of naphthopyran **186** with DDQ in the presence of allyl triphenyltin to form **187**. This reaction was extremely efficient and stereoselective, with no diastereomer being observed. A five-step sequence from **187** provided deoxyfrenolicin. Kim and Lee reported a bimolecular oxidative allylation reaction on an acyclic system that led to the synthesis of centrolobine.[102] Exposing benzylic ether **188** to DDQ and allyl tributyltin formed **189**. While the diastereocontrol was modest, this route nicely illustrated the power of oxidative carbon–hydrogen bond cleavage to form challenging ether linkages between two secondary carbons. Ring-closing metathesis and routine functional group interconversions provided the desired product.

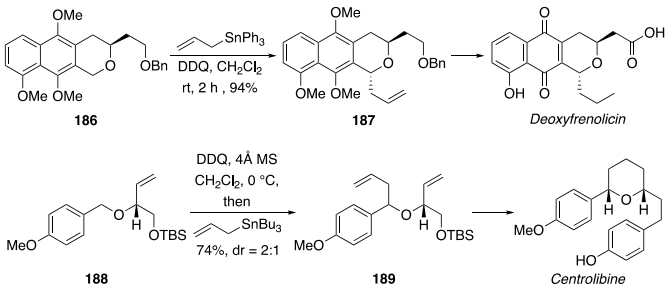

Scheme 37. Bimolecular oxidative allylation in natural product synthesis.

Tu showed that hydride abstraction is a viable strategy for incorporating oxocarbenium ions into macrocycles.[103] This strategy was used in the synthesis of neopeltolide (Scheme 38). Macrocyclic ether **190** reacts with DDQ to form bridged bicycle **191**. The alkene that is required for the oxidative cyclization can be removed through hydrogenation to set the proper stereochemical orientation of the methine group in the natural product. This alkene can also be functionalized in various ways to prepare analogs of the natural product.[104,105] Peh demonstrated an additional benefit of hydride abstraction-initiated cyclization reactions in the total synthesis of clavosolide A.[106] Cyclopropane-containing allylic ether **192** reacts with DDQ to form tetrahydropyran **193**. The stability of the cyclopropane group under these conditions is noteworthy since Lewis acid-mediated oxocarbenium ion generation is risky due to the potential for ionizing the tetrahydropyran in the product, leading to cyclopropane opening. The use of the enol acetate as the unsaturated group in this oxidation is also significant in demonstrating that functionalized alkenes can be

used to promote oxidation. Similarly, the conversion of **92** to **93** (Scheme 19) was a key step in the total synthesis of zampanolide.[70]

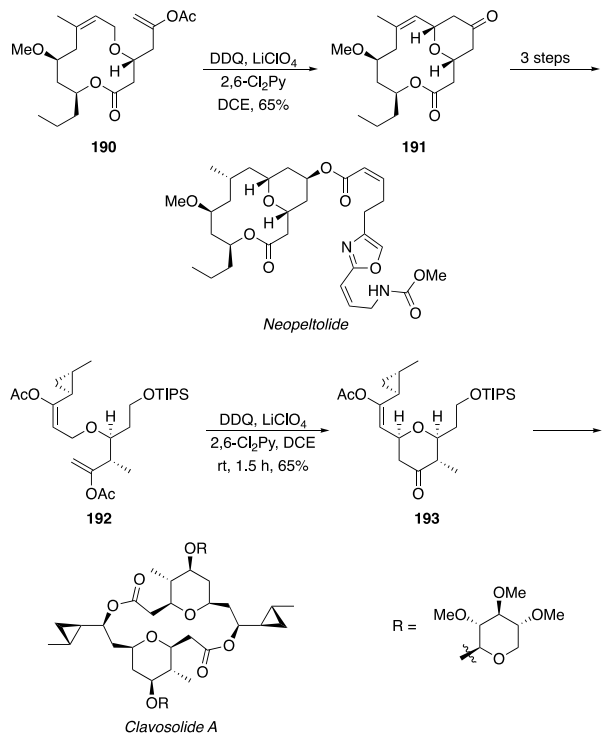

Scheme 38. Unique selectivity of oxidatively generated oxocarbenium ions in natural product syntheses.

Patir and Ertürk exploited the facility in which alkyl groups at the 3-position of indoles undergo hydride abstraction to form the bridged ring system of uleine (Scheme 39).[107] Oxidizing **194** generated a stable cation that reacts efficiently with an appended amide group to form **195**. Lu and co-workers utilized an indole oxidation in the synthesis of hapalindole H.[108] The cation that forms from the reaction of **196** and DDQ engages in a Prins reaction with an appended alkene to form **197**. This impressive report also demonstrated the scope of the oxidative Prins reaction on indole-derived carbocations and described the total syntheses of several members of the hapalindole family of natural products.

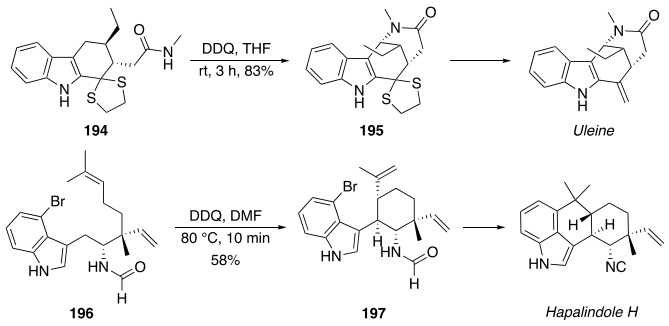

Scheme 39. Oxidation adjacent to indole in alkaloid synthesis.

Nitrogen-containing heterocycles in alkaloids can be manipulated or constructed through oxidative carbon–hydrogen bond cleavage, as illustrated in Scheme 40. Son and co-workers employed the facile oxidation of the tetrahydroisoquinoline nucleus in the synthesis of tetrabenazine.[109] The key reaction proceeded through the oxidation of **198** to form **199**, with the stereochemical outcome being consistent with the model shown in Scheme 26 for the conversion of **128** to **130**. The addition of a nitrogen-centered nucleophile to an oxidatively generated benzylic cation was the key step in the construction of the pyrrolidine unit of codonopsinol by Lingamurthy and co-workers.[110] Benzylic oxidation of **200**, while requiring elevated temperatures in the absence of a heteroatom stabilizing group, proceeded efficiently to deliver **201**. The authors propose that the high stereocontrol in this process arises from anchimeric assistance from the homobenzylic acetoxy group. The natural product is formed from acetoxy group cleavage and carbamate reduction.

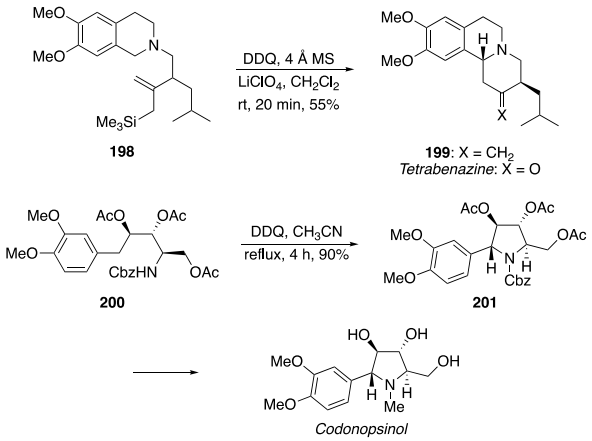

Scheme 40. Oxidative nitrogen heterocycle functionalization and formation.

Oxidative rearrangement pathways akin to the conversion of **183** to **185** in Scheme 36 have been exploited in complex molecule synthesis, as seen in Scheme 41. Jiao and co-workers applied this approach to the formal synthesis of platensimycin.[111] Ether **202** reacts with DDQ to form, after aldehyde reduction, bridged bicycle **203**, which was converted to **204**. Compound **204** has previously been converted to the natural product. Zhao and co-workers reported the total synthesis of brussonol from spirocyclic ether **205**.[100] Oxidation to **206** proceeded efficiently and minimal functional group interconversions were required to access the natural product.

Ju and Beaudry reported a highly innovative oxidative route to cephalotaxanine (Scheme 42).[112] This process converts furan **207** to the natural product upon exposure to DDQ. The authors proposed an electron transfer-based pathway that terminates in a transannular Mannich reaction. However, in accord with the well-developed reactivity profile of DDQ, we propose an alternative hydride-abstraction pathway that proceeds through the same Mannich reaction. Cleavage of the doubly benzylic

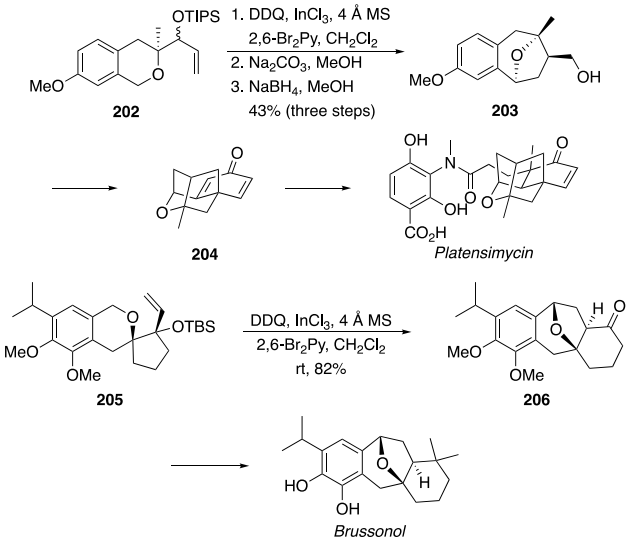

Scheme 41. Oxidative oxonia Cope/Prins cyclizations in natural product synthesis.

carbon–hydrogen leads to a carbocation that is additionally stabilized by the methoxy group on the furan. Addition of the amino group to the electron deficient heterocycle provides **208**. Breakdown of the aminal forms an enolate and an iminium ion (**209**) that allows for the transannular Mannich reaction to form the natural product.

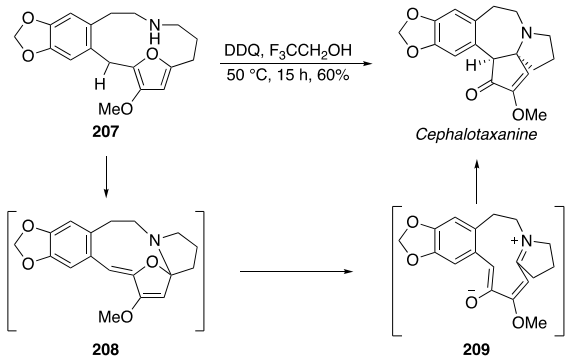

Scheme 42. Oxidative rearrangement to cephalotaxanine.

DDQ is effective in telescoped reactions in which the oxidation substrate is created through a bimolecular reaction, and this has been used in the synthesis of spirocyclic and bridged ring systems of natural products (Scheme 43). Han reported that the products of asymmetric hetero Diels-Alder reactions between silyloxy dienes and aldehydes are excellent substrates for oxidation by DDQ to form dihydropyrones. Appending a nucleophile creates the potential for further bond formation, as seen in the synthesis of bistramide A.[113] The hetero Diels-Alder reaction between **210** and **211** proceeds with Jacobsen's catalyst[114] to form **212**. Dilution with CH_2Cl_2 and oxidation with DDQ provides **213**, in which acid treatment leads to silyl ether cleavage and spirocyclization to deliver **214** in a convergent approach to spiroketals from acyclic precursors. A second-generation version of this approach was employed to prepare analogs through a more convergent pathway.[115] Caplan showed that bridged ketals are accessible by incorporating the nucleophile into the aldehyde fragment rather than the diene fragment and applied this to the synthesis of divergolide E.[116] The hetero Diels-Alder between diene **215** and aldehyde **216** provided, after oxidation, dihydropyrone **217**. While the requisite protecting group on the phenol was not compatible with a one-step bridged ketal construction, a subsequent transformation led to the formation of this subunit and, eventually, the natural product along with the acyl-migrated isomeric natural product divergolide H.

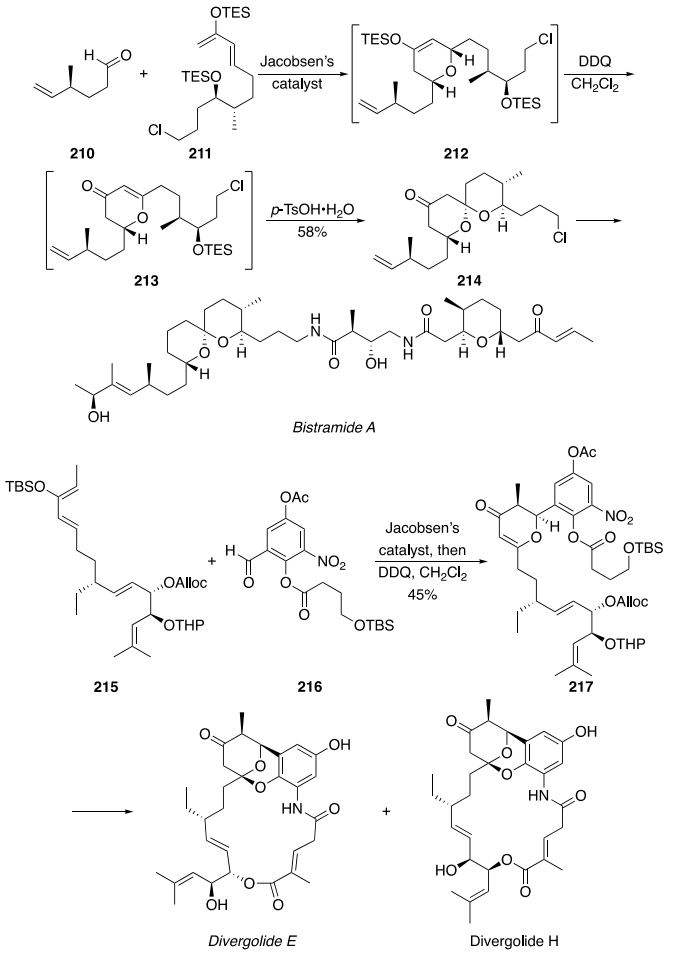

Scheme 43. Telescoped cycloadditions and oxidations in natural product synthesis.

6 Catalysis and asymmetric transformations

The benefits of employing DDQ in molecular synthesis are abundant, but limitations exist. DDQ-mediated oxidations inherently require the use of at least one equivalent, and often require super stoichiometric amounts to drive reactions to completion. Since DDQ is somewhat expensive, with a cost of >$550/mol from a common US supplier, and is modestly toxic, with an oral LD50 of 82 mg/kg in rats, numerous efforts have been directed at employing the reagent as a substoichiometric oxidant in conjunction with a more benign terminal oxidant that regenerates DDQ from $DDQH_2$ (**218**, Scheme 44). Additionally,

the flat geometry of DDQ precludes its use in enantioselective reaction development. Therefore current efforts in developing enantioselective DDQ-mediated bond forming processes focus on breaking the symmetry of the cationic intermediates that are generated through hydride transfer. This section will describe the efforts to address these fundamental limitations of DDQ.

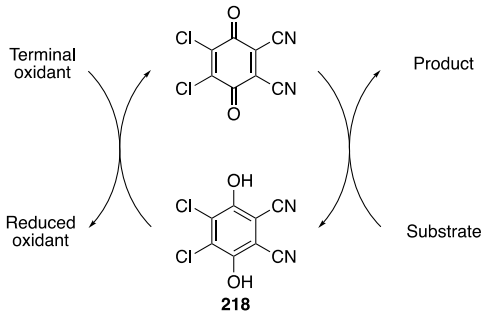

Scheme 44. Strategy for substoichiometric DDQ-mediated oxidations.

Chandrasekhar and co-workers took inspiration from the known oxidation of **218** to DDQ by non-toxic and inexpensive $FeCl_3$ in their design of a catalytic oxidative cleavage of PMB and DMB ethers (Scheme 45).[117] This protocol utilizes 10 mol% DDQ and 3 equiv $FeCl_3$, as seen in the conversion of **219** to **220**. No reaction occurs in the absence of DDQ, indicating that this is likely an oxidation reaction rather than a Lewis acid-mediated cleavage. However this attractive process has not been used for bond-forming reactions, perhaps as a consequence of the strong Lewis acidity of $FeCl_3$ in non-aqueous environments. Sharma and co-workers similarly showed PMB ether cleavage in the presence of 10 mol% DDQ and 3 equiv $Mn(OAc)_3 \bullet 2H_2O$,[118] and this reaction works well in the absence of added water. Functional group compatibility with this procedure is shown in the conversion of **221** to **222**. Although the cost of $Mn(OAc)_3 \bullet 2H_2O$ from commercial vendors is higher than the cost of DDQ, its minimal toxicity and rapid turnover rate make its use as a terminal oxidant an attractive option. Subsequent studies showed that this system is applicable to allylic and benzylic alcohol oxidation,[119] and to oxidative Nazarov[99] and Mannich-type reactions.[79]

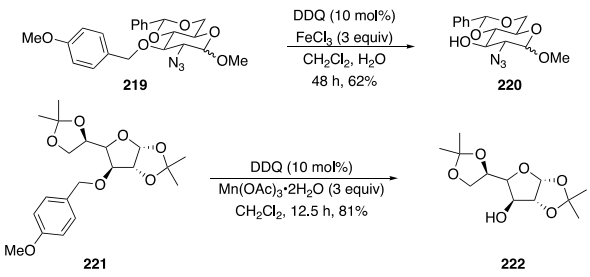

Scheme 45. Oxidative ether cleavage reactions with substoichiometric DDQ.

Liu showed that the exceedingly inexpensive oxidant MnO_2 can effect in situ DDQ regeneration in carbon–carbon bond forming reactions, as demonstrated by the conversion of **223** to **224** (Scheme 46).[120] Yields for these processes, which employed 15 mol% DDQ were good, though reaction times were much greater than similar transformations that utilized super stoichiometric quantities of DDQ. This most likely arises from the use of an insoluble terminal oxidant. Excess MnO_2 (6 equiv) is required, though the low cost and ease of purification through filtration make this a negligible concern. These conditions are also suitable for ether cleavage, oxidative acetal formation, and aromatization reactions, and subsequently were shown to be useful in oxidative Nazarov[99] and esterification processes.[121] Ghosh and Cheng reported that a similar cyclization can be accomplished by using ceric ammonium nitrate (CAN) as the terminal oxidant,[122] with the conversion of **225** to **226** serving as an excellent example. The cost of CAN is approximately half of the cost of DDQ, though two equivalents are required. The strength of the method is the relatively rapid rate, the low toxicity of CAN, and the ease of separation. Muramatsu and Nakano, building on their use of organometallic agents as nucleophiles for DDQ-generated electrophiles,[123] showed that $PhI(OTFA)_2$ can be used to regenerate DDQ.[124] This is seen in the conversion of isochroman **48** to **54**. While $PhI(OTFA)_2$ is significantly more expensive than DDQ, it regenerates the reagent quickly and could prove to be useful for purification purposes.

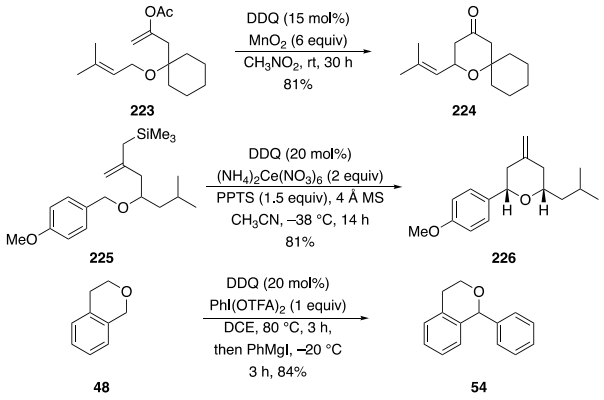

Scheme 46. DDQ-catalyzed oxidative carbon–carbon bond-forming reactions.

Numerous reports describe the use of dual catalytic aerobic DDQ-mediated oxidations in which transiently formed NO_2 serves as the direct oxidant of $DDQH_2$ (Scheme 47). These studies utilize *t*BuONO[125] or HONO[126] as a source of NO, which is converted to NO_2 by O_2. The oxidation of $DDQH_2$ to DDQ converts NO_2 to NO, and the cycle continues. Variations on the protocol employ photoirradiation,[127] which significantly enhances the rates of the processes, and HNO_3 as a source of NO_2 rather than NO.[128] These reactions are most commonly employed for benzylic and allylic alcohol oxidation and ether cleavage reactions, though Pan described an application to benzylic esterification[129] and Cheng reported oxidative carbon–carbon bond formation[130] using these protocols. Applications to carbon–carbon bond construction in densely functionally molecules has yet to be demonstrated, though the appeal of utilizing aerobic conditions to regenerate DDQ in situ dictates that these conditions should be considered in future reaction

design. Additional dual catalytic protocols combine DDQ with iron(II) phthalocyanine[131] or AIBN[132] under aerobic conditions.

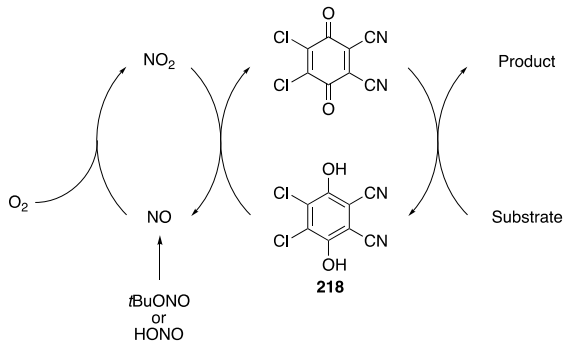

Scheme 47. Dual catalysis in aerobic DDQ-mediated oxidations.

DDQ can be regenerated under conditions that do not employ small molecules (Scheme 48). Kang and co-workers reported a synthesis of benzoxazoles in which $DDQH_2$ is converted to DDQ through an electrochemical oxidation.[133] Exposing imine **227** to substoichiometric DDQ at a constant current of 5 mA/cm^2 led to the formation of benzoxazole **228**. Ghorashi and co-workers showed that the enzyme laccase can regenerate DDQ under aerobic conditions.[134] Conversion of **229** to quinazolinone **230** proceeds with 20 mol% DDQ, laccase, and O_2 in high yield. The applicability of both protocols to bond-forming reactions has yet to be demonstrated but these efforts represent innovative strategies for mitigating the environmental impact of DDQ-mediated oxidations.

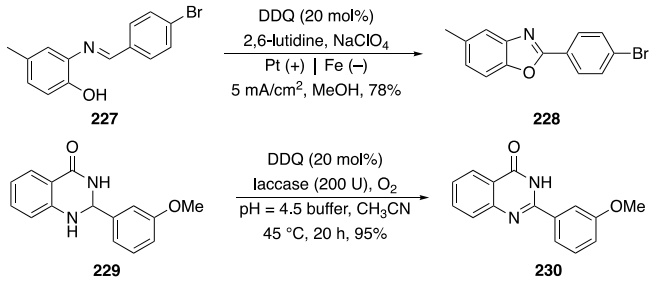

Scheme 48. Alternative methods for DDQ regeneration.

DDQ is planar and the cationic intermediates that it generates are generally not stereocenters. Therefore absolute stereocontrol is challenging, and most processes exploit relative stereocontrol. Strategies for controlling the absolute stereochemistry of the products focus on introducing asymmetry following the oxidation. This is most frequently achieved through generating chiral electrophiles or by the use of chiral nucleophiles A less common but creative alternative utilizes traceless stereoinduction.

Chiral electrophiles can be prepared via enamine oxidation. Hayashi and co-workers showed that transiently generated chiral enamines can be oxidized to form acyliminium ions (Scheme 49).[135] This is illustrated by the oxidation of **231** by DDQ in the presence of amine **232** (20 mol%) to generate enamine **233**. This creates a readily oxidized system that readily converts to iminium ion **234**. Nitromethane proceeds through a 1,4-addition upon completion of the oxidation, leading to the formation of **235** after the hydrolysis of the resulting enamine, resulting in a net asymmetric aldehyde β-functionalization reaction. Subsequent studies showed that the DDQ loading can be reduced to 10 mol% by using MnO_2 as the terminal oxidant with essentially no consequence to the yield or enantioselectivity.[136]

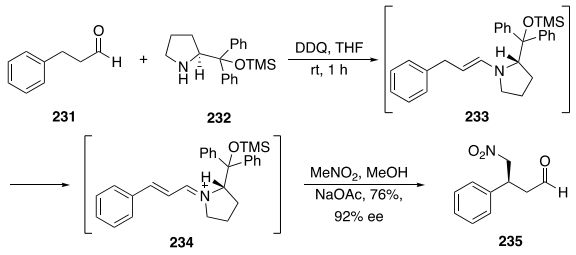

Scheme 49. Asymmetric aldehyde β-functionalization via enamine oxidation.

Cui and co-workers showed that chiral ion pairs can be formed when chromenes are oxidized in the presence of chiral Brønsted acids (Scheme 50).[137] This results from the exchange of $DDQH^-$ in the initially formed ion pair by a chiral anion. Oxidizing **236** in the presence of **237** (20 mol%) forms a chiral ion pair that reacts with allyl phenyldimethylsilane to form **238** in reasonable yield and enantioselectivity. However this process was quite limited in scope.

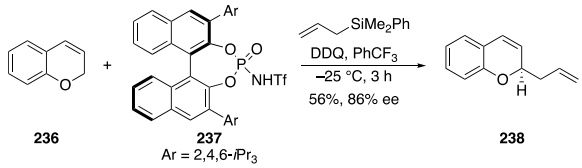

Scheme 50. Enantioselective allylation through a chiral ion pair.

Much broader scope is observed in the activation of oxidatively generated quinone methides (Scheme 51). Pan and co-workers showed that the oxidation of **239** by DDQ and MnO_2 produces quinone methide **240** that is activated by chiral phosphoric acid **241** (5 mol%) toward reaction with indole to form **242** in excellent yield and enantioselectivity.[138] The same group demonstrated that this pathway can be used for deracemization.[139] Oxidizing racemic **239** in the presence of **243** followed by the addition of Hantzch ester **244** results in the recovery of the starting material in high enantiomeric purity and yield. These processes show that the use of an achiral oxidant is useful in transforming racemic starting materials into identical chiral ion pairs. This strategy is also effective at deracemizing structurally diverse cyclic benzylic ethers.[140]

Benfatti and co-workers showed that chiral enamines can react with oxidatively generated carbocations to form products in good enantiomeric excess, thereby proving the value of utilizing chiral nucleophiles in these processes.[141] This is illustrated (Scheme 52) by the oxidation of xanthene (**245**) in

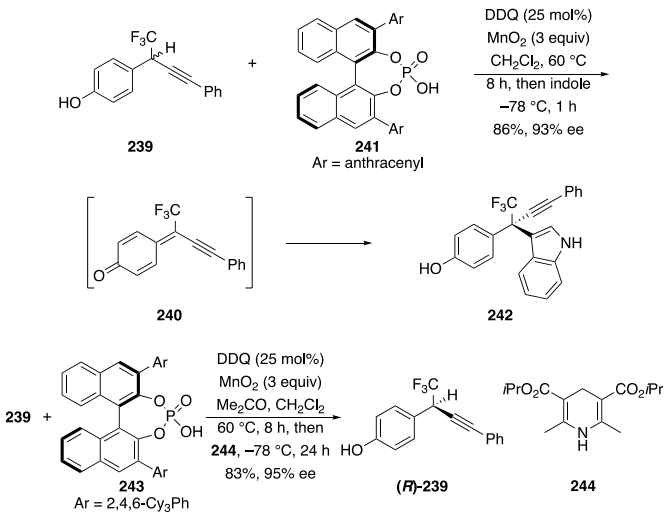

Scheme 51. Enantioselective additions to oxidatively generated quinone methides.

the presence of aldehyde **246** and a chiral amine catalyst to form **247**. Other readily oxidized substrates can serve as substrates though prochiral electrophiles led to the formation of diastereomeric mixtures. Similarly Meng and co-workers showed that chromans can serve as substrates for oxidative enamine additions, as shown by the oxidation of **48** by DDQ in the presence of aldehyde **231** and a chiral amine.[142] Reduction of the resulting aldehyde formed **248** in good yield, excellent enantioselectivity, and acceptable diastereoselectivity. Mechanistic studies showed that water was the initial nucleophile for the addition onto the intermediate oxocarbenium ion. This group also showed that dihydropyrans can serve as suitable substrates for this chemistry.[143]

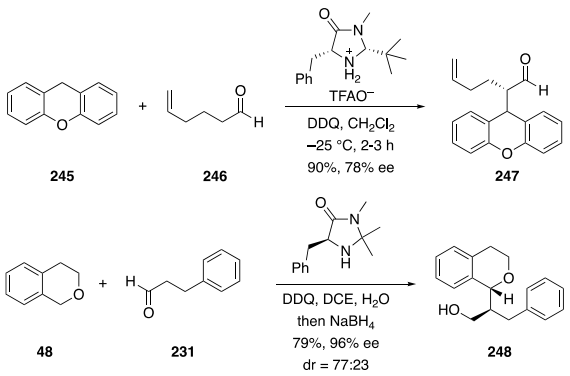

Scheme 52. Enantioselectivity with chiral enamine nucleophiles.

Asymmetric carbon–carbon bond formation with sp^2-hybridized carbons can be achieved through the use of chiral vinyl boronate intermediates (Scheme 53).[144] Adding DDQ to a mixture of *N*-acyl tetrahydropyridine **249** and **250** in the presence of a tartaric acid monoamide provides **251** in good yield and outstanding enantioselectivity. Alkoxy exchange between the ethoxy groups on **250** and the tartrate provides the reactive nucleophile, while oxidizing **249** in the presence of trifluoroethanol leads to the formation of an *N*,*O*-acetal that acts as a latent acyliminium ion.

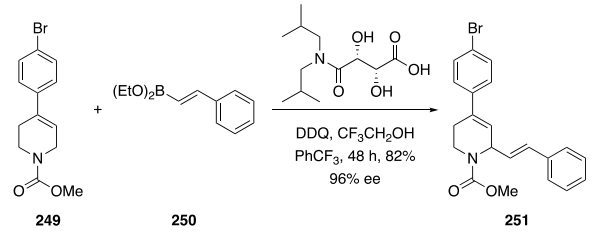

Scheme 53. Transiently generated chiral boronate as the nucleophile.

The acidifying capacity of copper-based Lewis acids can be exploited to generate enolates under mild conditions. Incorporating chiral ligands leads to enolates that can engage in asymmetric addition reactions. Zhang and co-workers showed that the iminium ion resulting from the oxidation of **252** reacts with **253** in the presence of $Cu(OTf)_2$ and ligand **254** to form Mannich product **255** in high yield and enantiomeric excess and with good diastereocontrol.[145] Lee showed that this strategy can be applied to intramolecular reactions in an enantioselective approach to tetrahydropyran synthesis.[146] Oxidizing keto ester **256** in the presence of Lewis acid **257** produces **258** in high yield and enantioselectivity. This approach is also effective with substituted keto esters that provide quaternary centers.

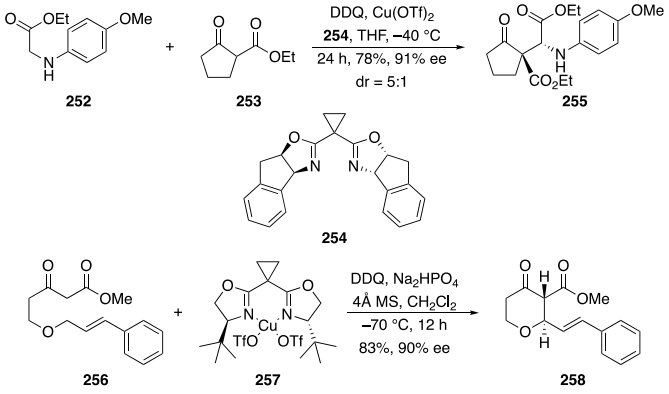

Scheme 54. Chiral enolate additions into oxidatively generated electrophiles.

Hu and co-workers reported an intriguing approach to using DDQ for an oxidation that produces a molecule with a single stereogenic unit in high enantiomeric excess.[147] This approach utilizes central chirality to influence the conformation of substrates that are axially chiral after oxidation. This is illustrated in Scheme 55, whereby the oxidation of enantiomerically enriched **259** (99% ee) provides **260** in 97% ee in a traceless approach to the synthesis of enantiomerically enriched substrates. This group also used a similar approach to prepare axially chiral naphthyl quinolines.[148]

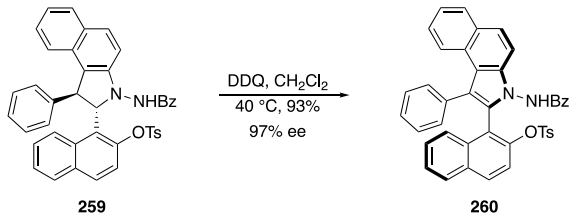

Scheme 55. Oxidative conversion of central to axial chirality.

C Oxoammonium Ions

1 Early Studies and Mechanistic Aspects

Oxoammonium ions contain a double bond between nitrogen and oxygen with a formal positive charge on nitrogen. The nitrogen is bonded to two carbons that are fully substituted or serve as bridging atoms in a bicyclic structure to prevent proton loss to form a nitrone. These compounds are readily accessible through oxidation or acid-promoted disproportionation of stable nitroxyl radicals. Common structures are shown in Figure 1, with the most frequently employed agents being those derived from TEMPO or its derivatives (**261**, **262**) and those derived from the bridged bicycle ABNO (**263**, **264**). Numerous variations on these structures have also been reported.

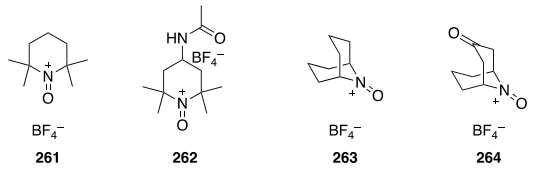

Figure 1. Common oxoammonium ion oxidants.

Oxoammonium ions most commonly served as alcohol oxidants in early applications.[149] Subsequent studies showed that incorporating inductively electron-withdrawing groups into the structures resulted in higher activity,[150,151] with compound **261** ($T^+BF_4^-$) being very convenient for many applications and compound **262** (known as Bobbitt's salt) showing a desirable profile from the perspective of reactivity, solubility, and ease of preparation.

Alcohol oxidations proceed most rapidly with sterically unencumbered alcohols at high pH, with primary alcohols generally reacting faster than secondary alcohols, while secondary alcohols generally react faster than primary alcohols at low pH or in non-aqueous solvents. Bailey and co-workers conducted a computational investigation of this divergent reactivity trend.[152] This work concluded that reactions at high pH proceed through a pathway in which the alcohol adds to the sterically hindered nitrogen atom to produce intermediate **265** (Figure 2), while reactions at low pH proceed through transition state **266** in a hydride-abstraction pathway. The need to form a complex between the alcohol and the sterically hindered nitrogen explains the steric selectivity, while the hydride abstraction pathway will be facilitated by the cation-stabilizing effect of increased substitution.

Figure 2. Alcohol oxidation under basic and acidic conditions.

The hydride abstraction mechanism indicates that these reagents can be used to oxidize ethers and related compounds. Pradhan and co-workers demonstrated the validity of this hypothesis through the use of Bobbitt's salt for the cleavage of benzylic ethers (Scheme 56).[153] Benzyl ether **267** can be oxidized to oxocarbenium ion **268**. Water in the solvent reacts to cleave the oxocarbenium ion to form benzaldehyde and release the alcohol, which can undergo further oxidation to form **269** since 2 equivalents of the oxidant were used. The successful application of these conditions to unsubstituted benzyl ethers indicates that Bobbitt's salt is a more potent oxidant than DDQ. Reactivity is enhanced by incorporating electron-donating groups on the arene and is completely inhibited in aliphatic ethers.

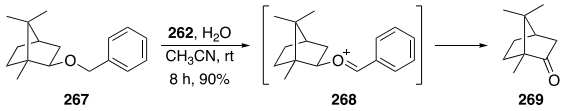

Scheme 56. Oxoammonium ion mediated benzyl ether cleavage through hydride abstraction.

Hamlin and co-workers conducted a computational study of the mechanism of ether oxidation by oxoammonium ions.[154] This study concluded that the process does occur through hydride abstraction and that substitutions on the arene in benzyl ethers alter the activation free energy in a manner that is consistent with a cation intermediate. Similarly, the ability of the oxygen to stabilize the cationic intermediate dictates reactivity, with alkoxy groups being more effective than phenoxy groups and significantly superior to acyloxy groups. This work also demonstrated that allylic ethers can be oxidized by Bobbitt's salt. The activation free energies in this work were higher than expected, most likely as a result of the calculated products having the (*Z*)-geometry for the oxocarbenium ion rather than the more favorable (*E*)-geometry. A subsequent investigation by Miller, Zhou, and co-workers showed[42] that transition state free energies more closely match experimental results when the reaction pathway provides the (*E*)-oxocarbenium ion, and that the rates of these reactions are generally much greater than those of corresponding oxidations by DDQ when both reactions are conducted in acetonitrile. This work also showed that, in contrast to DDQ reactions, oxidations

by oxoammonium ions are not sensitive to substrate oxidation potential and cation stability is the defining factor in hydride abstraction rates. The geometry of the hydride abstraction transition state places the sterically bulky geminal methyl groups distal to the oxidation site, making the processes less sensitive to steric effects in that region of the molecule than DDQ oxidations that require a stacked geometry. The conclusions of the mechanistic and computational studies are summarized in Figure 3.

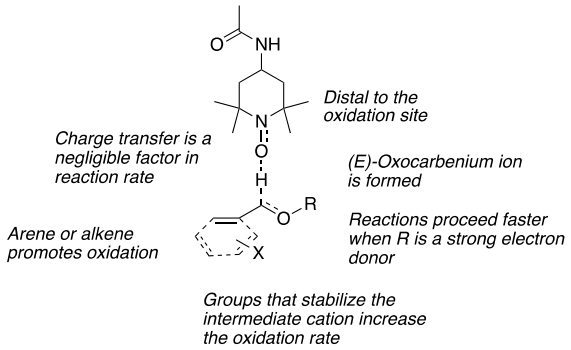

Figure 3. Summary of the influence of structural features on the transition state energy as determined computationally and experimentally.

2 Applications to Bond Forming Reactions

Reactions that employ oxoammonium ions for bond formation are relatively new entries in the toolbox of synthetic organic chemists and, therefore, have not been employed in the diverse applications that were developed with DDQ-mediated oxidations. These processes focus strongly on readily oxidized systems, with particular attention being directed to benzo-fused heterocycles such as tetrahydroisoquinolines and isochromans. However, as investigations progress to systems that proceed through challenging oxidations, a clear picture is emerging of the advantages of oxoammonium ions over DDQ.

Richter and García Mancheño showed (Scheme 57) that isochromans and *N*-aryl tetrahydroisoquinolines can be alkylated by malonates and related species in the presence of $Fe(OTf)_2$ upon oxidation with $T^+BF_4^-$ (**261**).[155] This is illustrated by the coupling of isochroman **270** with diethyl malonate to form **271**. Fang and co-workers reported that a similar oxidation can be used to initiate coupling with methyl-substituted aromatic heterocycles.[156] Exposing **272** to Bobbitt's salt in the presence of quinoline derivative **273** resulted in the formation of **274**, in which the nucleophile arises from tautomerization of **273** to its enamine isomer. A related oxidative alkylation with aldehyde-derived enols has also been reported (not shown).[157] Ring expansion is possible through conducting the oxidations in the presence of Me_3SiCHN_2.[158] This is illustrated by the conversion of **275** to **277** via intermediate **276**.

A subtle but important aspect of this type of oxidation employs *N*-acyl or *N*-sulfonyl benzo-fused heterocycles as substrates rather than highly reactive *N*-aryl analogs (Scheme 58). This allows for facile cleavage of the group on nitrogen,

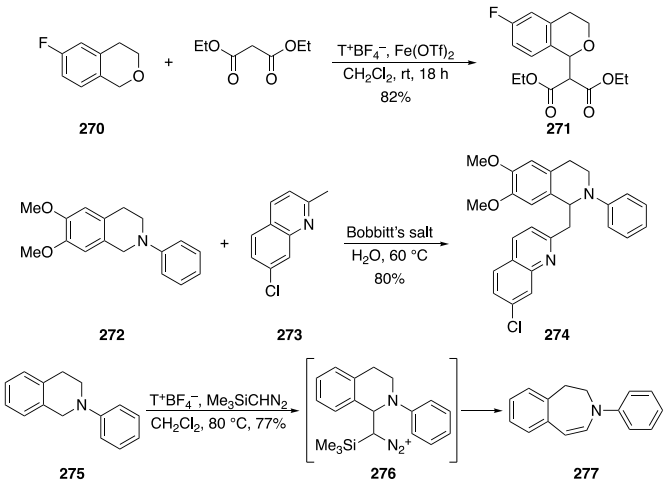

Scheme 57. Oxidation of benzo-fused heterocycles.

which is useful for numerous synthetic applications. The high reactivity of oxoammonium ions significantly facilitates this process. Yan and co-workers showed that *N*-sulfonyl tetrahydroisoquinoline **278** reacts with allyl trimethylsilane upon oxidation with $T^+BF_4^-$ to form **279**.[159] Sun and co-workers extended this chemistry for the functionalization of *N*-carboalkoxy tetrahydrocarbazoles.[160] Oxidation of **280** in the presence of vinyl trifluoroborate **281** forms **282** in good yield. *N*-Acyl dihydroquinolines are also excellent substrates for this process.[161] Added nitrogen incorporation can be achieved through the use of $TMSN_3$ as the nucleophile in the oxidation.[162]

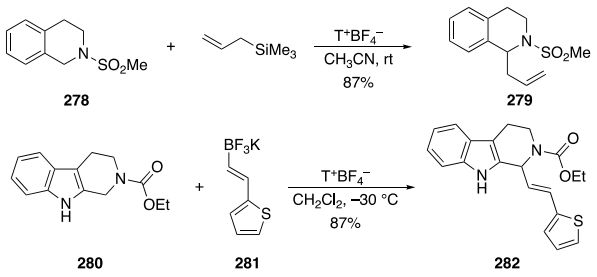

Scheme 58. Oxidative carbon–carbon bond formation from benzo-fused *N*-acyl heterocycles.

The high reactivity of oxoammonium ions allows for efficient oxidation of *N*-acyl heterocycles that do not have the energetic stabilization that benzo-fusion provides (Scheme 59). Wang and co-workers reported[163] that Boc-protected tetrahydropyridine **283** reacts with alkynyl trifluoroborate **284** in the presence of $T^+BF_4^-$ to provide **285** with excellent diastereocontrol. The trajectory of the nucleophile into the intermediate acyliminium ion can be reversed by incorporating the acyl group into a fused ring. Lactam **286** reacts with allyl trimethylsilane after oxidation by $T^+BF_4^-$ to produce **287**, again with excellent stereocontrol. This chemistry nicely extends an initial report in which non-alkylated *N*-acyl tetrahydropyridines were shown to be suitable

substrates for oxidative allylation, and that the unsaturation is necessary for reactivity.[159]

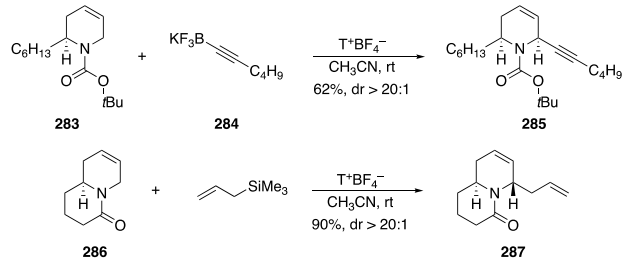

Scheme 59. Diastereoselective oxidative functionalizations of tetrahydropyridines.

Oxoammonium ions can be used to initiate oxidative annulation reactions (Scheme 60). An oxidative Povorov reaction occurs when amino ester **288** undergoes oxidation by $T^+BF_4^-$ in the presence of styrene and substoichiometric quantities of $FeCl_3$.[164] This initially produces **289**, which undergoes further oxidation to form quinoline **290**. This reaction is a six-electron oxidation, but only two equivalents of $T^+BF_4^-$ are required. The authors propose that the oxidative aromatization is accompanied by the reduction of the hydroxylamine product. Control studies showed that the $FeCl_3$ is important for promoting efficiency but its role is not addressed. An inverse electron demand formal [4+2] cycloaddition can be effected through the oxidation of benzylic carbamate **291** by Bobbitt's salt in the presence of styrene.[165] The authors propose that styrene adds into the intermediate acyliminium ion followed by the carbonyl group of the carbamate adding into the resulting benzylic cation to form **292**. Loss of the adamantyl cation leads to the final product **293**.

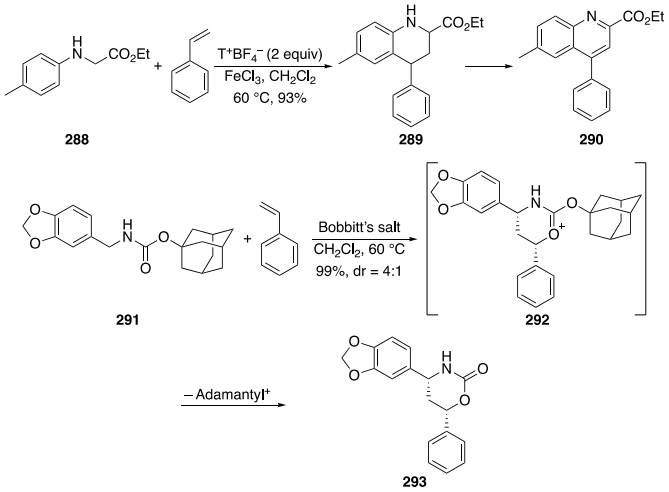

Scheme 60. Oxidative cycloadditions.

Oxidations of acyclic ethers can be more challenging than oxidations of cyclic substrates, but recent studies have demonstrated the feasibility of these processes (Scheme 61). Carlet and co-workers showed that cinnamyl ethers react with $T^+BF_4^-$ to form oxocarbenium ions.[166] Oxidizing ether **294** in the presence of allyl trimethylsilane provides allylation product **295**. Miller reported that Bobbitt's salt can act as a faster and less sterically sensitive substitute for DDQ in oxidative cyclization reactions that are similar to those shown in Scheme 18.[42] Exposing sterically hindered allylic ether **296** to Bobbitt's salt resulted in the formation of **297** in excellent yield. This study also showed that acyclic acyliminium ions can be prepared from oxidizing allylic carbamates with Bobbitt's salt. Liu and co-workers showed[167] that oxoammonium ions allow for a scope expansion of the oxidative oxonia Cope/aldol sequence that was introduced in Scheme 41. Ether **298** reacts with $T^+BF_4^-$ to form bridged bicycle **299**. This reaction did not proceed when DDQ was employed as the oxidant. N-Sulfonyl tetrahydropyridines can also serve as substrates for this process.

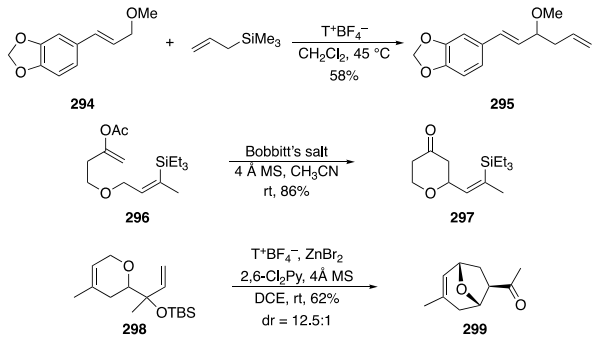

Scheme 61. Oxidative entry to acyclic oxocarbenium ions with oxoammonium ions.

3 Catalysis and asymmetric transformations

Numerous reagents can regenerate oxoammonium ions in alcohol oxidation reactions, including bleach,[168] CuCl and O_2,[169] *m*-CPBA,[170] Oxone and Bu_4NBr,[171] and $PhI(OAc)_2$.[172] Additionally electrochemical[173,174] and photoredox[175] conditions can be used to oxidized alcohols with catalytic quantities of nitroxyls. Despite these numerous successes, *in situ* oxoammonium ion regeneration is rare in hydride abstractions, with electrochemical oxidation being the only method that has thus far been employed. The schematic for this process is shown in Scheme 62, in which the oxoammonium ion is reduced by the substrate and re-oxidized by the anode. Nitroxyls can also be employed as an oxoammonium ion precursor since these

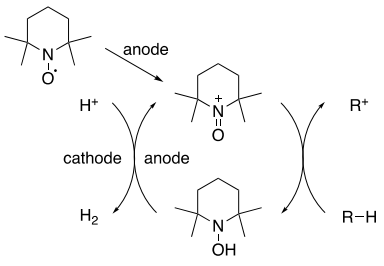

Scheme 62. Electrochemical oxoammonium ion regeneration.

species are readily oxidized at the anode. Chemical methods for oxoammonium ion regeneration commonly proceed under aqueous conditions and, therefore, are not compatible with carbon–carbon bond formation.

Kashiwagi showed that 4-benzoyloxy TEMPO (**300**) is an effective electrocatalyst for the oxidation of aromatic amines (Scheme 63).[176] Exposing amine **301** to **300** (10 mol%) in aqueous acetonitrile in a divided cell with $NaClO_4$ as the supporting electrolyte at a potential of 0.8 V vs Ag/AgCl provided formamide **302** in good yield. This results from the trapping of an intermediate iminium ion with water followed by a second oxidation of the aminal intermediate.

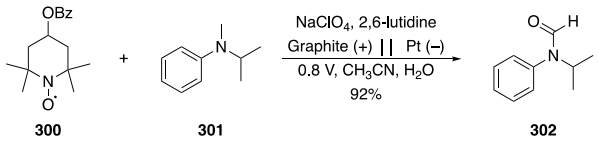

Scheme 63. Electrocatalytic amine oxidation.

Amides and carbamates are significantly more challenging to oxidize than amines due to the heightened instability of acyliminium ions. Wang and co-workers, however, showed that electrocatalytic Shono oxidations of carbamates derived from piperidines and pyrrolidines can be achieved with benzoyloxy ABNO (**303**) or ketoABNO (Scheme 64).[177] This is demonstrated by the conversion of carbamate **304** to **305**. Several aspects of these reactions are noteworthy. The loading of **303** is rather high, at 60 mol%, and more sterically hindered oxidants, such as Bobbitt's salt, are ineffective even in stoichiometric quantities. This indicates that the oxidation is quite challenging. The authors present evidence that the initial adduct arises from hydroxylamine addition into the intermediate acyliminium ion rather than water. While not addressed, this result and the steric sensitivity of the reaction suggest an alternative mechanism in which the oxygen atom of the oxoammonium ion inserts directly into the C–H bond. The use of a nitroxyl mediator in these reactions rather than a direct electrolysis allows for the incorporation of functional groups into the substrate that have similar oxidation potentials to the carbamate group and enhances site selectivity. Deprez and co-workers showed that the protocol can be extended to the oxidation of proline

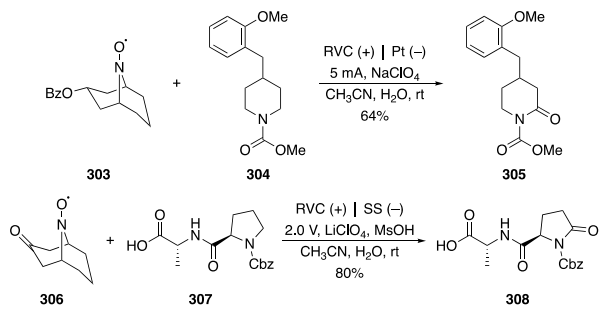

Scheme 64. Mediated Shono oxidations. RVS = reticulated vitreous carbon, SS = stainless steel.

derivatives and other pyrrolidines with multiple electron-withdrawing groups.[178] Keto ABNO (**306**) proved to be the optimal oxidant for these transformations, which are illustrated by the conversion of **307** to **308**. The reaction conditions were somewhat different for these reactions, with the major changes being the use of constant potential rather than constant current and the incorporation of MsOH as an additive. The compatibility of the method with a free carboxylic acid provides an additional illustration of the high degree of chemoselectivity for this process.

As previously discussed, oxidative carbon–carbon bond formation through oxoammonium ion-mediated hydride abstraction precludes the use of high concentrations of water in the solvent, thereby slowing electrochemical processes by diminishing the capacity of the cathode to release electrons. Additionally the products of carbon–carbon bond formation have a similar oxidation potential to the substrates, creating risks for decomposition via radical cation intermediates if the potential increases significantly. Lennox and co-workers addressed these issues in the cyanation of piperidines (Scheme 65).[179] The optimal oxidant for these reactions is ABNO (**309**), which can be used at 10-20 mol% loadings, and TMSCN is the cyanide source. The process is illustrated by the conversion of **310** to **311** (following protonation), in which the need for a proton source at the cathode was satisfied by the addition of 0.5 equiv. MeOH.

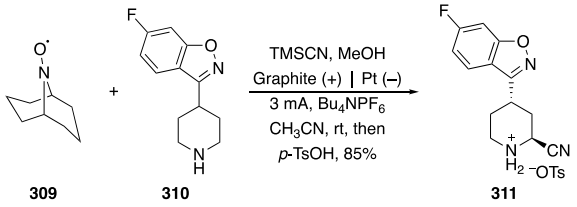

Scheme 65. Carbon–carbon bond formation through electrocatalytic C–H oxidation.

Ether oxidation is considerably slower than amine oxidation and, therefore, generates the hydroxylamine product in much lower concentrations. The low concentration of hydroxylamine leads to significant increases in potential when the reaction is conducted under constant current conditions, creating the possibility for substrate and product decomposition through single electron oxidation pathways. These problems were addressed by Lawrence,[180] who showed that constant potential conditions are desirable for these transformations where the potential is substantially higher than the oxidation potential of the hydroxylamine but lower than the oxidation potential of the substrate. Additionally, trifluoroethanol (TFE) is the optimal additive to ensure that the kinetics of oxidant regeneration are suitable for conducting the transformations in a reasonable time frame (Scheme 66). This is seen in the oxidative cyclization of **312** to **313** in which the loading of Bobbitt's salt can be lowered to 20 mol% from the 2 equiv. that are normally required for efficient reactions. Oxidations that are even slower can be conducted with stronger oxidants, and increasing the

concentrations of the reactions allows the oxoammonium ion loading to be lowered further.

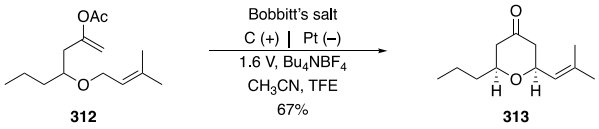

Scheme 66. Electrocatalytic ether oxidation.

Oxoammonium ions, unlike quinones, can be chiral due to the high sp^3-hybridized atom content in their structure. Several chiral nitroxyls have been prepared and used for oxidative kinetic resolutions of alcohols.[181-185] These agents have not been employed in a similar fashion for hydride-abstraction reactions, however. An examination of the transition state for oxoammonium ion-mediated hydride abstractions (Figure 3) shows that the steric bulk of the oxidant is distal to the reactive site, making oxidative kinetic resolutions in these processes an extremely challenging objective. Therefore asymmetric processes with oxoammonium ions, like DDQ, proceed through the use of chiral nucleophiles or chiral counterions for the electrophilic intermediates.

Sun and co-workers showed that alkynyl copper reagents, when coordinated to chiral ligands, can add into cations that arise from the oxidation of *N*-acyl tetrahydroisoquinolines (Scheme 67).[186] These processes employ multiple reagents in a single flask, as illustrated by the oxidative alkynylation of **314**. This process utilizes $T^+BF_4^-$ for hydride abstraction, then the resulting acyliminium ion is initially quenched with EtOH. Phenyl acetylene reacts with KOH, copper chloride, and ligand **315** to form a chiral nucleophile. The acyliminium ion is regenerated with $Yb(OTf)_3$ and the addition proceeds to form **316** with excellent enantioselectivity.

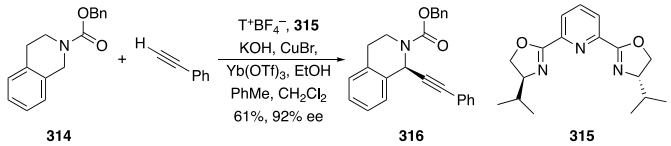

Scheme 67. Oxidative asymmetric alkynylation.

Utilizing chiral ion-pairing as a strategy for asymmetric induction in fast oxidations is challenging due to the potential for a racemic background reaction. Neel and co-workers addressed this issue through the use of a chiral phase-transfer catalyst that can carry Bobbitt's salt into a non-polar solvent for the enantioselective intramolecular addition of secondary amides to oxidatively generated carbocations (Scheme 68).[187] Bobbitt's salt is not soluble in toluene and can only oxidize tetrahydroisoquinoline **317** after anion exchange with the conjugate base of **318a** (5 mol%). The acid was identified based on a screen of a library of acids that was prepared though azide-alkyne cycloaddition reactions. This resulted in the formation of **319** in good yield and enantioselectivity. The absolute stereochemistry of the major product was not reported. A subsequent data intensive investigation[188] led to the identification of acid **318b** as a marginally superior agent for the cyclization of **317** but as a significantly improved additive for the cyclizations of other substrates. Biswas and co-workers advanced this strategy by showing that sulfide **320** can be oxidized in the presence of **321** to produce **322** with good enantiocontrol.[189] Mechanistic studies showed that the enantiodifferentiation step is cyclization rather than hydride abstraction.

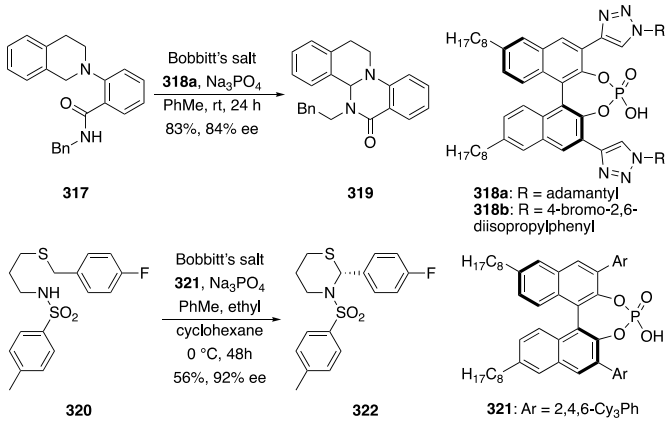

Scheme 68. Chiral phase-transfer catalysis in asymmetric oxidative cyclization reactions.

Gao and co-workers merged the use of a chiral nucleophile with electrochemical oxidant regeneration in the alkynylation of aryl tetrahydroisoquinolines and related species (Scheme 69).[190] Substrate **323** reacts with phenylacetylene in the presence of TEMPO (20 mol%), $Cu(OTf)_2$, ligand **324** and TFE under constant current conditions to yield **325** in good yield and excellent enantioselectivity. The same group reported that *N*-aryl glycine esters can undergo electrocatalytic, organocatalytic, enantioselective, oxidative Mannich reactions.[191] This process

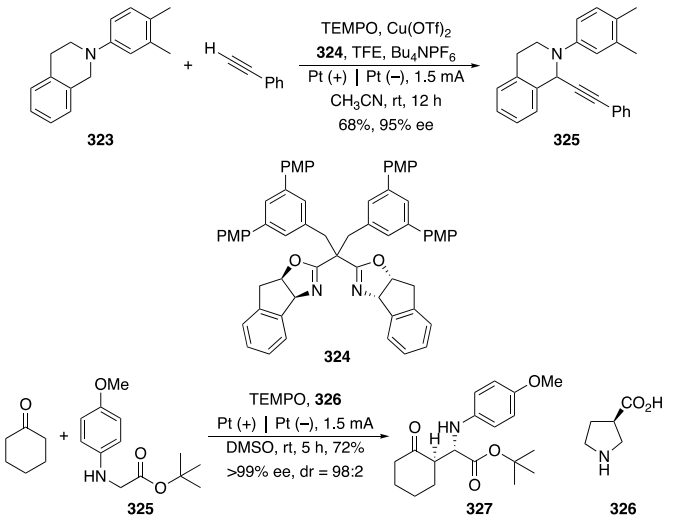

Scheme 69. Asymmetric electrocatalytic oxidative carbon–carbon bond forming reactions.

employs TEMPO as the pre-catalyst for the oxidation of amine **325** to produce the expected iminium ion. Condensation of cyclohexanone with organocatalyst **326** to generate a chiral enamine nucleophile. Coupling of the two species produces Mannich adduct **327** with exceptional stereocontrol.

D Carbocation oxidants

1 Early studies and mechanistic aspects

Isolable carbocations, such as variants on the trityl (triphenylmethyl, Tr^+ **328**) and tropylium (cycloheptatrienyl, **329**) ions (Figure 4), can be used as hydride abstracting agents. Trityl ions are considerably stronger oxidants than tropylium ions due to the aromatic stabilization that is present in the latter species, though both classes have been used in the development of oxidative carbon–carbon bond forming processes.

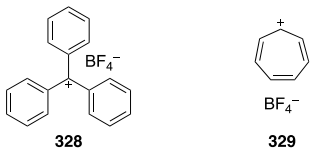

328 329

Figure 4. Common carbocation oxidants.

Initial studies with trityl ions focused on examinations of the structures that serve as suitable hydride donors. Dauben and co-workers showed (Scheme 70) that **328** can be generated *in situ* by treating triphenylmethanol with HBF_4.[192] Adding cycloheptatriene to the resulting cation leads to the formation of **329**, providing a clear illustration of the relative stabilities of the ions. Tertiary amines are excellent hydride donors,[193,194] with the oxidative conversion of **330** to acridinium ion **331**[195] being a notable example. The β-silicon effect makes tetraalkyl silanes effective reducing agents toward trityl cations.[196] Phenethyl trimethylsilane (**332**) reduces **328** to generate cation **333** and ultimately release styrene. This reaction is faster than the corresponding rection with tetraethyl silane by a factor of 779, indicating that cation stability is an important factor in

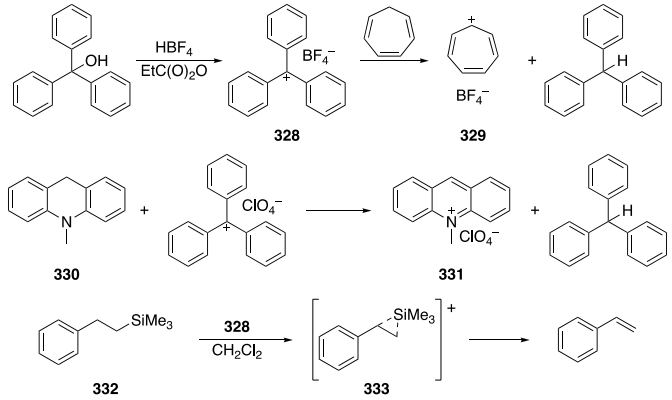

Scheme 70. Early examples of hydride transfer to the trityl cation.

determining the kinetics of trityl cation-based hydride abstractions.

Horn and co-workers initiated a program that was directed toward developing a universal hydride-donor scale.[197] Substituted and unsubstituted trityl and benzhydryl (diarylmethyl) cations were used as the hydride-abstracting agents in these studies and, consequently, substantial insights into the reactivities of these species became evident (Figure 5). Benzhydryl cations abstract hydrides at rates that exceed those of similarly substituted trityl cations by up to five orders of magnitude. Substituents on the arenes have the expected impact on hydride-abstraction reactivity, with electron-donating groups at the *para*-positions lowering reactivity, electron-withdrawing groups at the *para*-positions increasing reactivity, and electronegative groups at the *meta*-positions increasing reactivity. These processes indicated that the reactions can clearly be considered as hydride transfer processes. The authors observed a modest sensitivity to steric effects, with hydride transfer proceeding more rapidly from methylene groups than otherwise similarly substituted methine groups. Miller showed[42] that the trityl cation is significantly less sensitive than DDQ to steric effects distal to the reactive site. The calculated transition states for these reactions show that the aryl rings exist in a propeller arrangement that allows for remote steric effects to be avoided. This study showed that charge transfer is at most a minimal component of transition state free energy and that the trityl cation abstracts hydrides faster than Bobbitt's salt.

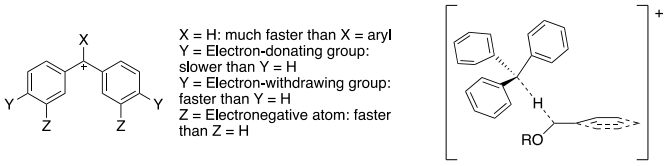

Figure 5. Reactivity trends and transition state geometry for trityl cation-mediated hydride abstraction.

The high reactivity of the trityl cation leads to alternative reaction pathways that, in certain cases, were initially interpreted as arising from hydride abstraction. This is seen in the cleavage of methylthiomethyl ether **334** by Ph_3CClO_4 (Scheme 71). This reaction was proposed to occur through a hydride abstraction in the initial report.[198] Niwa and Miyachi re-examined this process[199] and identified Ph_3CSMe as the by-product rather than the expected Ph_3CH, which is consistent with a report by Hashimoto and co-workers[200] that described the formation of stabilized carbocations by thiol abstraction. Additionally, Mayr and co-workers reported[201] that trityl cations can be alkylated by π-systems, indicating that the propensities

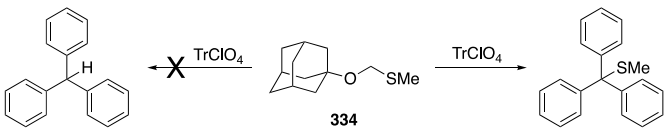

Scheme 71. Reaction of the trityl cation as a Lewis acid rather than a hydride-abstracting agent.

of trityl cations to undergo hydride abstraction and alkylation must be weighed in designing new reactions.

2 Synthetic studies

Barton and co-workers showed the utility of trityl cation-mediated oxidation reactions in numerous acetal and ketal cleavage reactions of complex molecules (Scheme 72).[202-204] Ether cleavage is illustrated through the conversion of PMB ether **335** with $TrBF_4$ to form, after the addition of water, cholesterol (**336**). The authors confirmed that the oxocarbenium ion intermediate formed through hydride abstraction by isolating triphenylmethane. Several variations on the substrate confirmed that intermediate cation stability controls the hydride-abstraction rate. Cyclic ketals of 1,2-diols also undergo hydride abstraction, as illustrated by the oxidation of **337**. This process was proposed to proceed through hydride abstraction that occurs in concert with ketal opening to form **338**. The addition of water forms hydroxy ketone **339**.

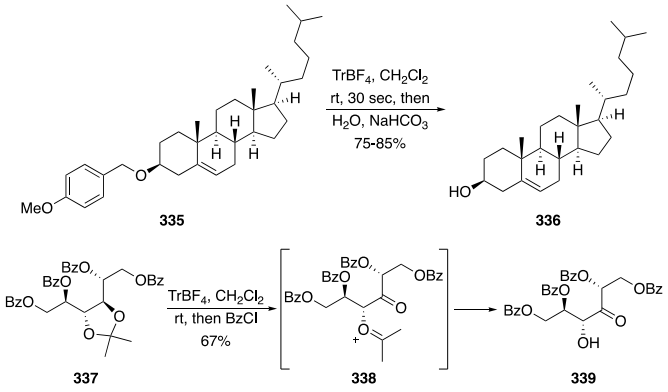

Scheme 72. Trityl cation-mediated protecting group manipulations.

Trityl ion-mediated hydride abstraction adjacent to highly electron-rich alkenes can be used for useful synthetic transformations (Scheme 73). Jung and co-workers showed that enolsilanes react with $TrBF_4$ to form enones.[205] Enolsilane **340** reacts to form cation **341**, which breaks down to form enone **342**. The mass recovery in these processes is quite good, with the only isolated products being the enone and the hydrolyzed enolsilane. The reaction also works for the formation of α,β-unsaturated esters from silyl ketene acetals. Hashimoto and Mukaiyama showed that the cations that form in the oxidation step can be used for carbon–carbon bond formation when a breakdown step is not available.[206,207] Ketene dithioacetal **343** or its isomeric allylic dithioacetal **344** are oxidized by $TrBF_4$ to form intermediate **345**. The addition of enolsilane **346** results in the formation of **347** through the equivalent of an oxidative Michael reaction. The isomeric starting materials deliver the products in nearly identical yields. Additional nucleophiles, including allylsilanes and prochiral enolsilanes are suitable for this reaction.

The oxidation of heterocyclic substrates is the most common application of trityl cations in bond-forming processes.

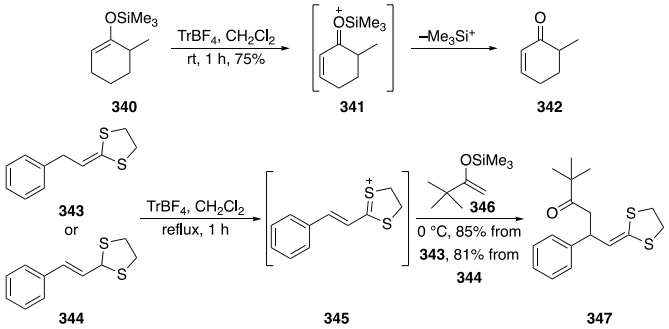

Scheme 73. Allylic oxidation of electron-rich alkenes.

Xie and co-workers showed that numerous unsaturated heterocyclic carbamates react to form acyliminium ions that can engage in bimolecular coupling reactions.[208] A representative example (Scheme 74) shows that the oxidation of tetrahydropyridine **348** in the presence of benzylic potassium trifluoroborate **349** cleanly produces **350**. A wide range of potassium trifluoroborate nucleophiles are suitable coupling partners with this protocol, including alkenyl, alkynyl, and aryl species, and ketones and aldehydes participate without the need for enolate generation. Good levels of stereocontrol can be achieved through the use of phenmenthol carbamates. Benzopyrans also participate in similar reactions.[209] The potency of trityl cations as hydride abstracting agents allows for the formation of electrophiles from substrates that are quite inert under most conditions.[210] 2-Methyl tetrahydrofuran can be oxidized by $TrGaCl_4$ (generated in situ from TrCl and $GaCl_3$) and coupled with alkynyl potassium trifluoroborates, as seen in the addition of **351** to form **352**. Regiocontrol is high for this reaction and is consistent with observations on the steric sensitivity of trityl cations toward substituents on the reactive site.[197]

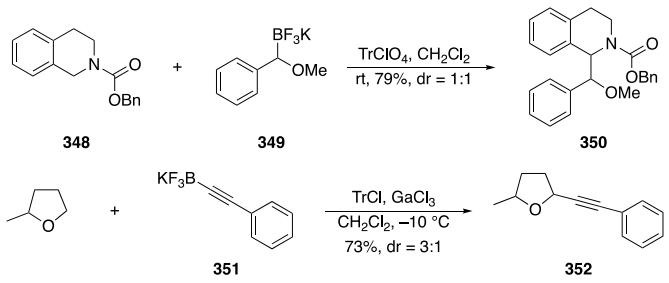

Scheme 74. Heterocycle oxidation with the trityl cation.

Oxidation with the trityl cation does not produce a Lewis basic product, and this proves to be beneficial in the development of sensitive multicomponent reactions that proceed through an electrophilic intermediate. Wang and co-workers demonstrated (Scheme 75) that their catalytic iron-mediated generation of nucleophiles is compatible with electrophiles that form through trityl cation-mediated hydride abstraction.[211] Alkyne **353** is converted to a nucleophilic

organoiron intermediate in the presence of an iron complex and *sym*-collidine, and this intermediate reacts with tetrahydropyridine **354** upon oxidation with $TrBF_4$ to form **355**. Allenes can also be used as precursors to the nucleophiles in these reactions.[212] Yesilcimen and co-workers employed the trityl cation to form dienophiles in asymmetric inverse electron-demand hetero Diels-Alder reactions from simple ethers.[213] Oxidizing tetrahydrofuran to form dihydrofuran in the presence of enone **356** and catalyst **357** results in the production of adduct **358** in excellent yield and with high stereocontrol. The use of TrOAc as the oxidant was necessary to maintain the concentration of trityl cation at a low level since it catalyzes a background racemic hetero Diels-Alder reaction. This process constitutes a rare example of asymmetric catalysis in a trityl cation-mediated transformation.

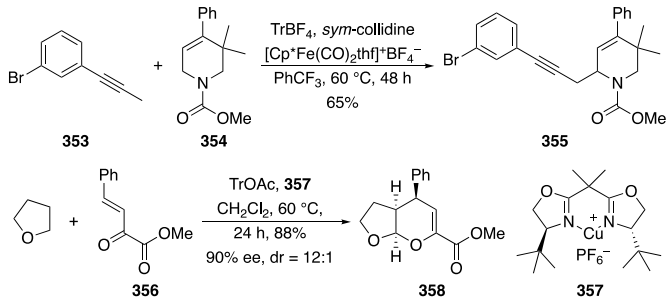

Scheme 75. Trityl cation oxidation in the presence of organometallic reagents.

The tropylium ion is a substantially weaker oxidant than the trityl cation, but it can serve as a mild agent for the oxidation of amines. This is shown by the work of Allen and Lambert,[214] in which oxidative cyanation of amines is reported (Scheme 76). Sparteine (**359**) reacts with tropylium tetrafluoroborate to form iminium ion **360**, which is quenched by cyanide to form **361**. Regioselectivity in these processes is not fully explained by cation stability or steric effects, and merits further exploration. A cursory examination of the reactions with various substrates suggests that the oxidant stacks on the substrate through either cation-π or van der Waals interactions, and the geometry of this complex dictates which hydrogen is sufficiently proximal to undergo abstraction.

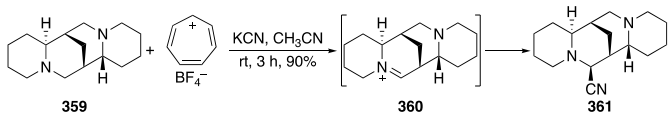

Scheme 76. Tropylium ion-mediated amine oxidation.

E Miscellaneous oxidants

The tropylium cation-mediated oxidations from the previous section demonstrate a utility for weak, selective oxidants in reaction development. This section covers the applications of two weak oxidants that show unique attributes. One will be used in the conversion of anions to neutral electrophiles, while the other will enable a hydride-borrowing strategy that enables the design of catalytic reactions that proceed through hydride abstraction.

Chen and co-workers showed[215] that ketones can oxidize lithium amides (Scheme 77) through a pathway that is similar to a Meerwein-Ponndorf-Verley reduction[216] and expands nicely on prior studies by Wittig and Hesse.[217] Deprotonating piperidine derivative **362** with *n*BuLi followed by treatment with PhC(O)*t*Bu provides imine **363**. A subsequent addition of an organolithium reagent and an aqueous quench delivers **364**, which is the natural product solenopsin A, in good yield and diastereoselectivity. The scope of this protocol can be expanded by adding pre-formed enolates,[218] enolates derived from β-keto acid decarboxylation,[219] or weaker nucleophiles in the presence of Lewis acids.[220] An intriguing advance was provided by the demonstration that the intermediate imines can be converted to nucleophiles through deprotonation. Deprotonation and oxidation of piperidine followed by deprotonation with LDA yields aza enolate **365**. Quenching with BnBr forms a new imine that reacts with BuLi to form **366** in a creative approach to α,β-difunctionalization of amines.[221]

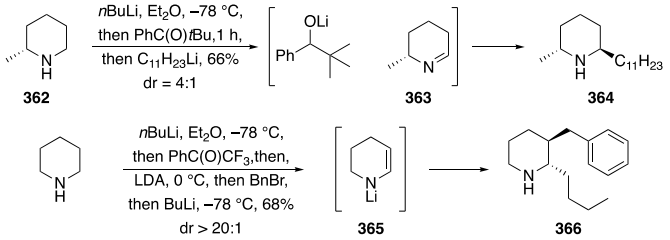

Scheme 77. Oxidation of lithium amides.

The Wasa group demonstrated the utility of $(F_5C_6)_3B$ as a weak oxidant that initially serves as a hydride acceptor and becomes an effective hydride donor. This is possible because the neutral borane is a weak oxidant that reacts only with readily oxidized hydride donors, making the resulting borohydride an effective reducing agent. The process is illustrated (Scheme 78) by the coupling of tertiary amine **367** with methyl acrylate to form **368**.[222] The amine is oxidized to form iminium ion **369** and the resulting borohydride reduces methyl acrylate to form enolate **370**. These species couple in a process that is redox neutral, allowing for the use of $(F_5C_6)_3B$ with a 5 mol% loading. The hydride borrowing approach can also be used for functionalizing the β-carbons of amines.[223] Raloxifene derivative **371** can be coupled to diisopropyl fumarate to form **372**. The route proceeds through hydride abstraction from **371** and proton loss from the resulting iminium ion to generate enamine **373**. Addition to the fumarate followed by reduction of iminium ion **374** completes the redox neutral transformation. This approach can also be used for β-deuteration with acetone-d_6 as a deuterium source.[224]

The ease in which hydride can be abstracted from triarylborohydrides allows for a sacrificial oxidant to be used for catalyst regeneration. This is illustrated (Scheme 79) by amine alkynylation.[225] Hydride abstraction from butenafine (**375**) by $(F_5C_6)_3B$ initiates coupling with ethyl trimethylsilylpropiolate in

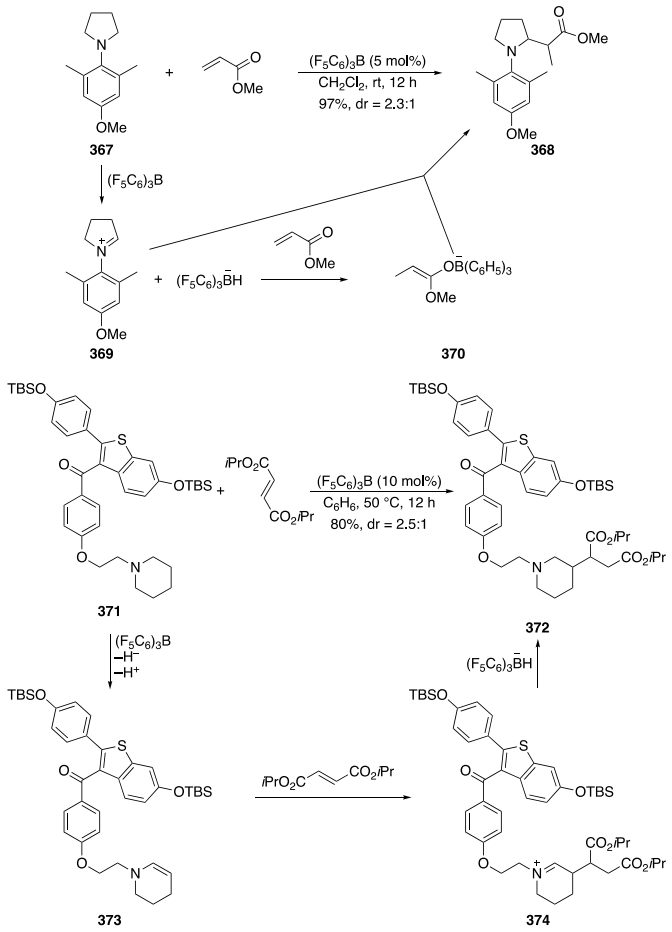

Scheme 78. Catalytic carbon–hydrogen bond functionalization through hydride borrowing.

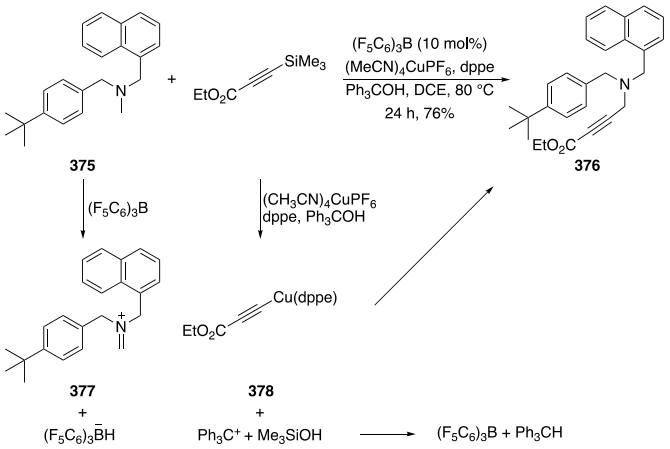

Scheme 79. Oxidative amine functionalization with a hydride-abstracting catalyst.

the presence of $(MeCN)_4CuPF_6$, 1,2-diphenylphosphinoethane (dppe), and Ph_3COH to form **376**. This reaction proceeds through one pathway in which the substrate is oxidized to iminium ion **377** and a separate pathway in which the alkyne is converted to copper reagent **378** with the resulting trimethylsilyl group sequestering the hydroxy group from Ph_3COH to form the trityl cation. The addition of **378** to **377** yields **376**, while the trityl cation regenerates the borane, or potentially continues the cycle by abstracting a hydride from the substrate. Good levels of enantiocontrol can be observed at prochiral carbons when a chiral ligand is used. This process is a net oxidation, but the low cost of Ph_3COH as a terminal oxidant makes this an attractive process. A conceptually related process can be employed for enolsilane nucleophiles.[226]

Conclusions

The application of organic hydride-abstracting agents has become a powerful approach to organic synthesis by providing strategy-level oxidation reactions from relatively less functionalized substrates. These processes are characterized by broad substrate scope that enhance their applicability in late-stage functionalization processes. The substantial advances that have been made in the development of these reactions have been described in the review, but new opportunities arise from prior successes. These are unique to each oxidant class.

Reactions that utilize quinone oxidants, particularly DDQ, are much better developed than reactions that use other oxidant classes. The reactivity patterns for DDQ are well-defined, but the need remains for a protocol that allows for its *in-situ* regeneration by inexpensive terminal oxidants that promote rapid turnover without generating by-products that could be detrimental to chemoselectivity. Advances in the development of asymmetric reactions that utilize DDQ provide guidance on the design of enantioselective transformations in processes that use an achiral oxidant and proceed through planar intermediates. Incorporating chiral ion pairs or chiral nucleophiles into oxidative bond-forming reactions defines an exciting frontier for these reactions.

The breadth of substrates that have been utilized in oxoammonium ion-mediated hydride abstractions is far less developed in comparison to the scope of DDQ-mediated oxidation reactions, but the foundations for understanding the reactivity patterns of these agents has emerged and this is essential in the design of future transformations. These agents abstract hydrides at rates that are greater than what is observed with DDQ, and ample opportunities exist for developing oxidative reactions that take advantage of this high reactivity. The development of asymmetric transformations with these agents follows the strategies that were employed with DDQ in the use of chiral ion-pairing agents and chiral nucleophiles. The potential for utilizing the potential for chiral oxoammonium ions for enantioselective reaction design has yet to be exploited for hydride-abstraction reactions, making this an intriguing area for further investigation. Electrochemical approaches to oxoammonium ion regeneration have been effective for lowering the loadings of these somewhat expensive reagents, and efforts need to continue for developing electrocatalytic variants of slower reactions in non-aqueous solvents.

Trityl cations, while being introduced as hydride-abstracting agents decades ago, have not found wide use in reaction

development. However their unique attribute of lacking any basic functional group after serving as an oxidant is attractive for applications in processes that merge transition metal catalysis with hydride abstraction, and this has recently been demonstrated. The reactivity of these agents can also be easily and rationally adjusted by incorporating substituents on the arenes, and this could prove to be useful for enhancing chemoselectivity.

Weaker hydride-abstracting agents, including ketones and triaryl boranes, have recently proved to offer unique attributes to oxidative bond forming reactions. The weaker oxidation capacities can be useful in hydride abstractions of anions, whereby deprotonation can serve as a route to highly chemoselective oxidations. Additionally, the ease by which triaryl borohydrides can be oxidized has created a new area of catalytic hydride borrowing transformations. These agents demonstrate that abundant opportunities exist for creative advances in this active area of research.

Conflicts of interest

There are no conflicts to declare.

Acknowledgements

This work was supported by generous funding from the National Science Foundation (CHE-1855877).

Notes and references

1 T. Newhouse, P. S. Baran and R. W. Hoffmann, *Chem. Soc. Rev.* 2009, **38**, 3010-3021.
2 B. M. Trost, *Science*, 1991, **254**, 1471-1477.
3 P. A. Wender, V. A. Verma, T. J. Paxton and T. H. Pillow, *Acc. Chem. Res.*, 2008, **41**, 40-49.
4 N. Z. Burns, P. S. Baran and R. W. Hoffmann, *Angew. Chem., Int. Ed.* 2009, **48**, 2854-2867.
5 W. Ali, G. Prakash and D. Maiti, *Chem. Sci.*, 2021, **12**, 2735-2759.
6 N. Y. S. Lam, K. Wu and J.-Q. Yu, *Angew. Chem., Int. Ed.*, 2021, **60**, 16767-15790.
7 Q. Zhang and B.-F. Shi, *Chem. Sci.*, 2021, **12**, 841-852.
8 R. Narayan, K. Matcha and A. P. Antonchick, *Chem. Eur. J.*, 2015, **21**, 14678-14693.
9 D. J. Abrams, P. A. Provencher and E. J. Sorensen, *Chem. Soc. Rev.*, 2018, **47**, 8925-8967.
10 M. C. White and J. Zhao, *J. Am. Chem. Soc.*, 2018, **140**, 13988-14009.
11 N. Sauerman, T. H. Meyer, Y. Qiu and L. Ackerman, *ACS Catal.*, 2018, **8**, 7086-7103.
12 T. Gensch, M. N. Hopkinson, F. Glorius and J. Wencel-Delord, *Chem. Soc. Rev.*, 2016, **45**, 2900-2936.
13 Z. Huang, H. N. Lim, F. Mo, M. C. Young and G. Dong, *Chem. Soc. Rev.*, 2015, **44**, 7764-7786.
14 D. Y.-K. Chen and S. W. Youn, *Chem. Eur. J.*, 2012, **18**, 9452-9474.
15 W. R. Gutekunst and P. S. Baran, *Chem. Soc. Rev.*, 2011, **40**, 1976-1991.
16 For a recent review on the chemistry of quinones, see: A. E. Wendlandt and S. S. Stahl, *Angew. Chem., Int. Ed.*, 2015, **54**, 14638-14658.
17 E. A. Braude, L. M. Jackman, R. P. Linstead and G. Lowe, *J. Chem. Soc.*, 1960, 3123-3132.
18 A. M. Creighton and L. M. Jackman, *J. Chem. Soc.*, 1960, 3138-3144.
19 K. Horita, T. Yoshioka, T. Tanaka, Y. Oikawa and O. Yonemitsu, *Tetrahedron*, 1986, **42**, 3021-3028.
20 C. Hansch, A. Leo and R. W. Taft, *Chem. Rev.*, 1991, **91**, 165-195.
21 W. Zhang, H. Ma, C.-C. Li and W.-M. Dai, *Tetrahedron*, 2019, **75**, 1795-1807.
22 J. S. Yadav, S. Chandrasekhar, G. Sumithra and R. Kache, *Tetrahedron Lett.*, 1996, **37**, 6603-6606.
23 J.-M. Vatèle, *Tetrahedron*, 2002, **58**, 5689-5698.
24 B. M Trost, *J. Am. Chem. Soc.*, 1967, **89**, 1847-1851.
25 H. H. Jung and P. E. Floreancig, *Tetrahedron*, 2009, **65**, 10830-10836.
26 H.-D. Becker, *J. Org. Chem.*, 1965, **30**, 982-989.
27 O. R. Shehab and A. M. Mansour, *J. Mol. Struct.* 2013, **1047**, 121-135.
28 R. M. Scribner, *J. Org. Chem.*, 1966, **31**, 3671-3682.
29 H. G. Roth, N. A. Romero and D. A. Nicewicz, *Synlett*, 2016, **27**, 714-723.
30 A. K. Turek, D. J. Hardee, A. M. Ullman, D. G. Nocera and E. N. Jacobsen, *Angew. Chem., Int. Ed.*, 2016, **55**, 539-544.
31 C. Höfler and C. Rüchardt, *Liebigs Ann.*, 1996, 183-188.
32 B. Chan and L. Radom, *J. Phys. Chem. A*, 2007, **111**, 6456-6467.
33 O. R. Luca, T. Wang, S. J. Konezny, V. S. Batista and R. H. Crabtree, *New J. Chem.*, 2011, **35**, 998-999.
34 X. Guo, H. Zipse and H. Mayr, *J. Am. Chem. Soc.*, 2014, **136**, 13863-13873.
35 S. Yamabe, S. Yamazaki and S. Sasaki, *Int. J. Quantum Chem.*, 2015, **115**, 1533-1542.
36 C. A. Morales-Rivera, P. E. Floreancig and P. Liu, *J. Am. Chem. Soc.*, 2017, **139**, 17935-17944.
37 N. P. Schepp and L. J. Johnston, *J. Am. Chem. Soc.*, 1996, **118**, 2872-2881.
38 L. Liu and P. E. Floreancig, *Org. Lett.*, 2009, **11**, 3152-3155.
39 M. S. Sigman, K. C. Harper, E. N. Bess and A. Milo, *Acc. Chem. Res.*, 2016, **49**, 1292-1301.
40 S. M. Hubig, R. Rathore and J. K. Kochi, *J. Am. Chem. Soc.*, 1999, **121**, 617-626.
41 L. Liu and P. E. Floreancig, *Angew. Chem., Int. Ed.*, 2010, **49**, 3069-3072.
42 J. L. Miller, L. Zhou, P. Liu and P. E. Floreancig, *Chem. Eur. J.*, 2022, **28**, e202103078.
43 Y. Hayashi and T. Mukaiyama, *Chem. Lett.*, 1987, 1811-1814.
44 J.-i. Yoshida and S. Suga, *Chem. Eur. J.*, 2002, **8**, 2650-2658.
45 B.-P. Ying, B. G. Trogden, D. T. Kohlman, S. X. Liang and Y.-C. Xu, *Org. Lett.*, 2004, **6**, 1523-1526.
46 S. A. Girard, T. Knauber and C.-J. Li, *Angew. Chem., Int. Ed.*, 2014, **53**, 74-100.
47 Y. Zhang and C.-J. Li, *J. Am. Chem. Soc.*, 2006, **128**, 4242-4243.
48 Y. Zhang and C.-J. Li, *Angew. Chem., Int. Ed.*, 2006, **45**, 1949-1952.
49 S. J. Park, J. R. Price and M. H. Todd, *J. Org. Chem.*, 2012, **77**, 949-955.
50 M. Cao, Y. Mao, H. Huang, Y. Ma and L. Liu, *Tetrahedron Lett.*, 2019, **60**, 1075-1078.
51 Y. Mao, M. Cao, X. Pan, J. Huang, J. Li, L. Xu and L. Liu, *Org. Chem. Front.*, 2019, **6**, 2028-2031.
52 D. J. Clausen and P. E. Floreancig, *J. Org. Chem.*, 2012, **77**, 6574-6582.
53 A. S.-K. Tsang and M. H. Todd, *Tetrahedron Lett.*, 2009, **50**, 1199-1202.

54 A. S.-K. Tsang, P. Jensen, J. M. Hook, A. S. K. Hashmi and M. H. Todd, *Pure Appl. Chem.*, 2011, **83**, 655-665.
55 W. Su, J. Yu, Z. Li and Z. Jiang, *J. Org. Chem.*, 2011, **76**, 9144-9150.
56 H. Wang, X. Li, F. Wu and B. Wan, *Tetrahedron Lett.*, 2012, **53**, 681-683.
57 J. Ravindran, V. O. Yadhukrishnan, R. S. Asha and R. S. Lankalapalli, *Org. Biomol. Chem.*, 2020, **18**, 3927-3937.
58 C. A. Correia and C.-J. Li, *Adv. Synth. Catal.*, 2010, **352**, 1446-1450.
59 D. Cheng and W. Bao, *Adv. Synth. Catal.*, 2008, **350**, 1263-1266.
60 H. Mo and W. Bao, *Adv. Synth. Catal.*, 2009, **351**, 2845-2849.
61 Q. Chen, C. Wen, X. Wang, G. Tu, Y. Ou, Y. Huo and K. Zhang, *Adv. Synth. Catal.*, 2018, **360**, 3590-3594.
62 D. Cheng, M. Wang, Z. Deng, X. Yan, X. Xu and J. Yan, *Eur. J. Org. Chem.*, 2019, 4589-4592.
63 D. Cheng, Z. Deng, X. Yan, M. Wang, X. Xu and J. Yan, *Adv. Synth. Catal*., 2019, **361**, 5025-5029.
64 D. Cheng, X. Yan, Y. Pu, J. Shen, X. Xu and J. Yan, *Eur. J. Org.* Chem., 2021, 944-950.
65 W. Tu, L. Liu and P. E. Floreancig, *Angew. Chem., Int. Ed*., 2008, **47**, 4184-4187.
66 B. Yu, T. Jiang, J. Li, Y. Su, X. Pan and X. She, *Org. Lett.*, 2009, **11**, 3442-3445.
67 C. Olier, M. Kaafarani, S. Gastaldi and M. P. Bertrand, *Tetrahedron*, 2010, **66**, 413-445.
68 E. A. Crane and K. A. Scheidt, *Angew. Chem., Int. Ed.*, 2010, **49**, 8316-8326.
69 X. Han, G. Peh and P. E. Floreancig, *Eur. J. Org. Chem.*, 2013, 1193-1208.
70 A. K. Ghosh and X. Cheng, *Org. Lett*., 2011, **13**, 4108-4111.
71 B. V. Subba Reddy, P. Borkar, J. S. Yadav, P. P. Reddy, A. C. Kunwar, B. Sridhar and R. Grée, *Org. Biomol. Chem.*, 2012, **10**, 1349-1358.
72 L. Liu and P. E. Floreancig, *Angew. Chem., Int. Ed.*, 2010, **49**, 3069-3072.
73 J. L. Broeker, R. W. Hoffmann and K. N. Houk, *J. Am. Chem. Soc.*, 1991, **113**, 5006-5017.
74 L. Liu and P. E. Floreancig, *Angew. Chem., Int. Ed.*, 2010, **49**, 5894-5897.
75 M. P. Castaldi, D. M. Troast and J. A. Porco, Jr., *Org. Lett.*, 2009, **11**, 3362-3365.
76 K. M. McQuaid and D. Sames, *J. Am. Chem. Soc.*, 2009, **131**, 402-403.
77 X.-H. Hu, F. Liu and T.-P. Loh, *Org. Lett.* 2009, **11**, 1741-1743.
78 X. Han and P. E. Floreancig, *Org. Lett*., 2012, **14**, 3808-3811.
79 G. J. Brizgys, H. H. Jung and P. E. Floreancig, *Chem. Sci.*, 2012, **3**, 438-442.
80 A. Kar, B. Chakraborty, S. Kundal, G. Rana and U. Jana, *Org. Biomol. Chem.*, 2021, **19**, 906-910.
81 S. Kundal, B. Chakraborty, K. Paul and U. Jana, *Org. Biomol. Chem.*, 2019, **17**, 2321-2325.
82 A. J. Grenning, J. K. Snyder and J. A. Porco, Jr., *Org. Lett.*, 2014, **16**, 792-795.
83 A. Jung and S.-J. Min, *Asian J. Org. Chem.*, 2019, **8**, 1617-1620.
84 H. Jo, A. H. E. Hassan, S. Y. Jung, J. K. Lee, Y. S. Cho and S.-J. Min, *Org. Lett.*, 2018, **20**, 1175-1178.
85 Y. Cui and P. E. Floreancig, *Org. Lett.*, 2012, **14**, 1720-1723.
86 H. Wang, Y.-L. Zhao, L. Li, S.-S. Li and Q. Liu, *Adv. Synth. Catal.*, 2014, **356**, 3157-3163.
87 J. Hubert, D. P. Furkert and M. A. Brimble, *J. Org. Chem.*, 2015, **80**, 2715-2723.
88 G. R. Peh and P. E. Floreancig, *Org. Lett.*, 2015, **17**, 3750-3753.
89 B. C. Lemercier and J. G. Pierce, *Org. Lett.*, 2015, **17**, 4542-4545.
90 P. D. Parker and J. G. Pierce, *Synthesis*, 2016, **48**, 1902-1909.
91 H. Yu, R. Lee, H. Kim and D. Lee, *Org. Lett.*, 2021, **23**, 1135-1140.
92 X. Wen, X. Li, X. Luo, W. Wang, S. Song and N. Jiao, *Chem. Sci.*, 2020, **11**, 4482-4487.
93 C. Qi, H. Cong, K. J. Cahill, P. Müller, R. P. Johnson and J. A. Porco, Jr., *Angew. Chem., Int. Ed.*, 2013, **52**, 8345-8348.
94 L. Zhou, B. Xu and J. Zhang, *Angew. Chem., Int. Ed.*, 2015, **54**, 9092-9096.
95 S. Manna and A. P. Antonchick, *Chem. Eur. J.*, 2017, **23**, 7825-7829.
96 H.-X. Feng, Y.-Y. Wang, J. Chin and L. Zhou, *Adv. Synth. Catal.*, 2015, **357**, 940-944.
97 W.-L. Xu, H. Zhong, Y.-L. Hu, H. Yang and L. Zhou, *Org. Lett.*, 2018, **20**, 5774-5778.
98 W.-L. Xu, W.-M. Zhao, M. Wang, J. Chen and L. Zhou, *Org. Lett.*, 2020, **22**, 7169-7174.
99 R. J. Fradette, M. Kang and F. G. West, *Angew. Chem., Int. Ed.*, 2017, **56**, 6335-6338.
100 Z.-W. Zhao, Y.-Q. Tu, Q. Zhang, W.-X. Liu, S.-Y. Zhang, S.-H. Wang, F.-M. Zhang and S. Jiang, *Nat. Commun*., 2015, **6**, 7332.
101 Y.-C. Xu, D. T. Kohlman, S. X. Liang and C. Erikkson, *Org. Lett.*, 1999, **1**, 1599-1602.
102 H. Kim and D. Lee, *Synlett*, 2015, **26**, 2583-2587.
103 W. Tu and P. E. Floreancig, *Angew. Chem., Int. Ed*., 2009, **48**, 4567-4571.
104 Y. Cui, W. Tu and P. E. Floreancig, *Tetrahedron*, 2010, **66**, 4867-4873.
105 Y. Cui, R. Balachandran, B. W. Day and P. E. Floreancig, *J. Org. Chem.*, 2012, **77**, 2225-2235.
106 G. R. Peh and P. E. Floreancig, *Org. Lett.*, 2012, **14**, 5614-5617.
107 S. Patir and E. Ertürk, *J. Org. Chem.*, 2011, **76**, 335-338.
108 Z. Lu, M. Yang, P. Chen, X. Xiong and A. Li, *Angew. Chem., Int. Ed.*, 2014, **53**, 13840-13844.
109 Y. W. Son, T. H. Kwon, J. K. Lee, A. N. Pao, J. Y. Lee, Y. S. Cho and S.-J. Min, *Org. Lett.*, 2011, **13**, 6500-6503.
110 M. Lingamurthy, Y. Jagadeeth, K. Ramakrishna and B. V. Rao, *J. Org. Chem.*, 2016, **81**, 1367-1377.
111 Z.-W. Zhao, Y.-Q. Tu, Q. Zhang, W.-X. Liu, S.-H. Wang and M. Wang, *Org. Chem. Front*., 2015, **2**, 913-916.
112 X. Ju and C. M. Beaudry, *Angew. Chem., Int. Ed.*, 2019, **58**, 6752-6755.
113 X. Han and P. E. Floreancig, *Angew. Chem., Int. Ed.*, 2014, **53**, 11075-11078.
114 A. G. Dossetter, T. F. Jamison and E. N. Jacobsen, *Angew. Chem., Int. Ed.*, 1999, **38**, 2398-2400.
115 R. D. Hanna, Y. Naro, A. Deiters and P. E. Floreancig, *Chem. Eur. J.*, 2018, **24**, 16271-16275.
116 S. M. Caplan and P. E. Floreancig, *Angew. Chem., Int. Ed.*, 2018, **57**, 15866-15870.
117 S. Chandrasekhar, G. Sumithra and J. S. Yadav, *Tetrahedron Lett.*, 1996, **37**, 1645-1646.
118 G. V. M. Sharma, B. Lavanya, A. K. Mahalingam and P. R. Krishna, *Tetrahedron Lett.*, 2000, **41**, 10323-10326.
119 C. C. Cosner, P. J. Cabrera, K. M. Byrd, A. M. A. Thomas and P. Helquist, *Org. Lett.*, 2011, **13**, 2071-2073.
120 L. Liu and P. E. Floreancig, *Org. Lett.*, 2010, **12**, 4686-4689.
121 Y. Hong, Q. Liu, J. Liu, Z. Zeng, Y. Yang, A. Lei, *ChemSusChem*, 2012, **5**, 2143-2146.
122 A. K. Ghosh and X. Cheng, *Tetrahedron Lett.*, 2012, **53**, 2568-2570.
123 W. Muramatsu, K. Nakano and C.-J. Li, *Org. Lett.*, 2013, **15**, 3650-3653.
124 W. Muramatsu and K. Nakano, *Org. Lett.*, 2014, **16**, 2042-2045.
125 Z. Shen, J. Dai, J. Xiong, X. He, W. Mo, B. Hu, N. Sun and X. Hu, *Adv. Synth. Catal.*, 2011, **353**, 3031-3038.

126 K. Walsh, H. F. Sneddon and C. J. Moody, *Tetrahedron*, 2014, **70**, 7380-7387.
127 K. Walsh, H. F. Sneddon and C. J. Moody, *Org. Lett.*, 2014, **16**, 5224-5227.
128 T. Katsina, L. Clavier, J.-F. Giffard, N. Macedo, P. da Silva, J. Fournier, R. Tamion, C. Copin, S. Arseniyadis and A. Jean, *Org. Process Res. Dev.*, 2020, **24**, 856-860.
129 D. Pan, Z. Pan, Z. Hu, M. Li, X. Hu, L. Jin, N. Sun, B. Hu and Z. Shen, *Eur. J. Org. Chem.*, 2019, 5650-5655.
130 D. Cheng, K. Yuan and J. Yan, *Tetrahedron Lett.*, 2015, **56**, 1641-1644.
131 Y. Hong, T. Fang, M. Li, Z. Shen, X. Hu, W. Mo, B. Hu, N. Sun and L. Jin, *RSC Adv.*, 2016, **6**, 51908-51913.
132 K. Alagiri, P. Devadig and K. R. Prabhu, *Chem. Eur. J.*, 2012, **18**, 5160-5164.
133 L.-S. Kang, H.-I. Xiao, C.-C. Zeng, L.-M. Hu and R. D. Little, *J. Electroanal. Chem.*, 2016, **767**, 13-17.
134 N. Ghorashi, Z. Shokri, R. Moradi, A. Abdelrasoul and A. Rostami, *RSC Adv*., 2020, **10**, 14254-14261.
135 Y. Hayashi, T. Itoh and H. Ishikawa, *Angew. Chem., Int. Ed.*, 2011, **50**, 3920-3924.
136 Y. Hayashi, T. Itoh and H. Ishikawa, *Adv. Synth. Catal.*, 2013, **355**, 3661-3669.
137 Y. Cui, L. A. Villafane, D. J. Clausen and P. E. Floreancig, *Tetrahedron*, 2013, **69**, 7618-7626.
138 X. Pan, Z. Wang, L. Kan, Y. Mao, Y. Zhu and L. Liu, *Chem. Sci.*, 2020, **11**, 2414-2419.
139 Y. Mao, Z. Wang, G. Wang, R. Zhao, L. Kan, X. Pan and L. Liu, *ACS Catal.*, 2020, **10**, 7785-7791.
140 M. Wan, S. Sun and L. Liu, *Angew. Chem., Int. Ed.*, 2017, **56**, 5116-5120
141 F. Benfatti, M. Capdavelia, L. Zoli, E. Benedetto and P. G. Cozzi, *Chem. Commun.*, 2009, 5919-5921.
142 Z. Meng, S. Sun, H. Yuan, H. Lou and L. Liu, *Angew. Chem., Int. Ed.*, 2013, **53**, 543-547.
143 X. Xin, X. Pan, Z. Meng, X. Liu and L. Liu, *Org. Chem. Front.*, 2019, **6**, 1448-1452.
144 X. Liu, Z. Meng, C. Li, H. Lou and L. Liu, *Angew. Chem., Int. Ed.*, 2015, **54**, 6012-6015.
145 G. Zhang, Y. Zhang and R. Wang, *Angew. Chem., Int. Ed.*, 2011, **50**, 10429-10432.
146 A. Lee, R. C. Betori, E. A. Crane and K. A. Scheidt, *J. Am. Chem. Soc.*, 2018, **140**, 6212-6216.
147 Y.-L. Hu, Z. Wang, H. Yang, J. Chen, Z.-B. Wu, Y. Lei and L. Zhou, *Chem. Sci.*, 2019, **10**, 6777-6784.
148 S.-J. Wang, Z. Wang, Y. Tang, J. Chen and L. Zhou, *Org. Lett.*, 2020, **22**, 8894-8898.
149 E. G. Rozantsev and V. D. Sholle, *Synthesis*, 1971, 401-414.
150 T. Miyazawa, T. Endo, S. Shiihashi and M. Okawara, *J. Org. Chem.*, 1985, **50**, 1332-1344.
151 J. M. Bobbitt, *J. Org. Chem.*, 1998, **63**, 9367-9374.
152 W. F. Bailey, J. M. Bobbitt and K. B. Wiberg, *J. Org. Chem.*, 2007, **72**, 4504-4509.
153 P. P. Pradhan, J. M. Bobbitt and W. F. Bailey, *J. Org. Chem.*, 2009, **74**, 9524-9527.
154 T. A. Hamlin, C. B. Kelly, J. M. Ovian, R. J. Wiles, L. J. Tilley and N. E. Leadbeater, *J. Org. Chem.*, 2015, **80**, 8150-8167.
155 H. Richter and O. García Mancheño, *Eur. J. Org. Chem.*, 2010, 4460-4467.
156 L. Fang, Z. Li, Z. Jiang, Z. Tan and Y. Xie, *Eur. J. Org. Chem.*, 2016, 3559-3567.
157 H. Richter, R. Rohlman and O. García Mancheño, *Chem. Eur. J.*, 2011, **17**, 11622-11627.
158 A. Gini, J. Bamberger, J. Luis-Barrera, M. Zurro, R. Mas-Ballestė, J. Alemán and O. García Mancheño, *Adv. Synth. Catal.*, 2016, **358**, 4049-4056.
159 C. Yan, Y. Liu and Q. Wang, *Org. Lett.*, 2015, **17**, 5714-5717.
160 Y. Sun, G. Wang, J. Chen, C. Liu, M. Cai, R. Zhu, H. Huang, W. Li and L. Liu, *Org. Biomol. Chem.*, 2016, **14**, 9431-9438.
161 Z. Liu, L. Chen, J. Li, J. Zhao, L. Feng, R. Wan, W. Li and L. Liu, *Org. Biomol. Chem.*, 2017, **15**, 7600-7606.
162 J. Dong, Q. Xia, H. Song, Y. Liu and Q. Wang, *J. Org. Chem.*, 2018, **83**, 4516-4524.
163 G. Wang, Y. Mao and L. Liu, *Org. Lett.*, 2016, **18**, 6476-6479.
164 H. Richter and O. García Mancheño, *Org. Lett.*, 2011, **13**, 6066-6069.
165 H. Richter, R. Frölich, C.-G. Daniliuc and O. García Mancheño, *Angew. Chem., Int. Ed.*, 2012, **51**, 8656-8660.
166 F. Carlet, G. Bertarini, G. Broggini, A. Pradal and G. Poli, *Eur. J. Org. Chem.*, 2021, 2162-2168.
167 P. L. Anelli, C. Biffi, F. Montanari and S. Quici, *J. Org. Chem.*, 1987, **52**, 2559-2562.
168 L. Liu, H.-L. Cheng, W.-Q. Ma, S.-H. Hou, Y.-Q. Tu, F.-M. Zhang, X.-M. Zhang and S.-H. Wang, *Chem. Commun.*, 2018, **54**, 196-199
169 M. F. Semmelhack, C. R. Schmid, D. A. Cortés and C. S. Chou, *J. Am. Chem. Soc.*, 1984, **106**, 3374-3376.
170 J. A. Cella, J. A. Kelley and E. F. Kenehan, *J. Org. Chem.*, 1975, **40**, 1860-1862.
171 C. Bolm, A. S. Magnus and J. P. Hildebrand, *Org. Lett.*, 2000, **2**, 1173-1175.
172 A. De Mico, R. Margarita, L. Parlanti, A. Vescovi and G. Piancatelli, *J. Org. Chem.*, 1997, **62**, 6974-6977.
173 M. F. Semmelhack, C. S. Chou and D. A. Cortes, *J. Am. Chem. Soc.*, 1983, **105**, 4492-4494.
174 M. Rafiee, K. C. Miles and S. S. Stahl, *J. Am. Chem. Soc.*, 2015, **137**, 14751-14757.
175 J. Nandi, J. M. Ovian, C. B. Kelly and N. E. Leadbeater, *Org. Biomol. Chem.*, 2017, **15**, 8295-8301.
176 Y. Kashiwagi and J.-i. Anzai, *Chem. Pharm. Bull.*, 2001, **49**, 324-326.
177 F. Wang, M. Rafiee and S. S. Stahl, *Angew. Chem., Int. Ed.*, 2018, **57**, 6686-6690.
178 N. R. Deprez, D. J. Clausen, J.-X. Yan, F. Peng, S. Zhang, J. Kong and Y. Bai, *Org. Lett.*, 2021, **23**, 8334-8337.
179 A. J. J. Lennox, S. L. Goes, M. P. Webster, H. F. Koolman, S. W. Djuric and S. S. Stahl, *J. Am. Chem. Soc.*, 2018, **140**, 11227-11231.
180 J.-M. I. A. Lawrence and P. E. Floreancig, *Chem. Eur. J.*, 2022, **28**, Early View.
181 S. D. Rychnovsky, T. L. McLernon and H. Rajapakse, *J. Org. Chem.*, 1996, **61**, 1194-1195.
182 Y. Kashiwagi, F. Kurashima, C. Kikuchi, J.-i. Anzai, T. Osa and J. M. Bobbitt, *Tetrahedron Lett.*, 1999, **40**, 6469-6472.
183 H. Shiigi, H. Mori, T. Tanaka, Y. Demizu and O. Onomura, *Tetrahedron Lett.*, 2008, **49**, 5247-5251.
184 S. Hamada, Y. Wada, S. Sasamori, N. Tokitoh, T. Furura and T. Kawabata, *Tetrahedron Lett.*, 2014, **55**, 1943-1945.
185 K. Murakami, Y. Sasano, M. Tomizawa, M. Shibuya, E. Kwon and Y. Iwabuchi, *J. Am. Chem. Soc.*, 2014, **136**, 17591-17600.
186 S. Sun, C. Li, P. E. Floreancig and L. Liu, *Org. Lett.*, 2015, **17**, 1684-1687.
187 A. J. Neel, J. P. Hehn, P. F. Tripet and F. D. Toste, *J. Am. Chem. Soc.*, 2013, **135**, 14044-14047.
188 A. Milo, A. J. Neel, F. D. Toste and M. S. Sigman, *Science*, 2015, **347**, 737-743.
189 S. Biswas, K. Kubota, M. Orlandi, M. Turberg, D. H. Miles, M. S. Sigman and F. D. Toste, *Angew. Chem., Int. Ed.*, 2018, **57**, 589-593.
190 P.-S. Gao, X.-J. Weng, Z.-H. Wang, C. Zheng, B. Sun, Z.-H. Chen, S.-L. You and T.-S. Meng, *Angew. Chem., Int. Ed.*, 2020, **59**, 15254-15259.

191 Z.-H. Wang, P.-S. Gao, X. Wang, J.-Q. Gao, X.-T. Xu, Z. He, C. Ma and T.-S. Mei, *J. Am. Chem. Soc.*, 2021, **143**, 15599-15605.
192 H. J. Dauben, Jr., L. R. Honnen and K. M. Harmon, *J. Org. Chem.*, 1960, **25**, 1442-1445.
193 R. Damico and C. D. Broaddus, *J. Org. Chem.*, 1966, **31**, 1607-1612.
194 H. Volz and H. H. Kiltz, *Tetrahedron Lett.*, 1970, **11**, 1917-1920.
195 M. Ishikawa, S. Fukuzumi, T. Goto and T. Tanaka, *Bull. Chem. Soc. Jpn.*, 1989, **62**, 3754-3756.
196 S. S. Washburne and R. Szendroi, *J. Org. Chem.*, 1981, **46**, 691-693.
197 M. Horn, L. H. Schappele, G. Lang-Wittkowski, H. Mayr and A. R. Ofial, *Chem. Eur. J.*, 2013, **19**, 249-263.
198 P. K. Chowdhury, R. P. Sharma and J. N. Baruah, *Tetrahedron Lett.*, 1983, **24**, 4485-4486.
199 H. Niwa and Y. Miyachi, *Bull. Chem. Soc. Jpn.*, 1991, **64**, 716-718.
200 Y. Hashimoto, H. Sugumi, T. Okauchi and T. Mukaiyama, *Chem. Lett.*, 1987, **16**, 1691-1694.
201 H. Mayr, G. Lang and A. R. Ofial, *J. Am. Chem. Soc.*, 2002, **124**, 4076-4083.
202 D. H. R. Barton, P. D. Magnus, G. Smith and D. Zurr, *J. Chem. Soc. D*, 1971, 861-863.
203 D. H. R. Barton, P. D. Magnus, G. Streckert and D. Zurr, *J. Chem. Soc. D*, 1971, 1109-1111.
204 D. H. R. Barton, P. D. Magnus, G. Smith, G. Streckert and D. Zurr, *J. Chem. Soc., Perkin Trans. 1*, 1972, 542-552.
205 M. E. Jung, Y.-G. Pan, M. W. Rathke, D. F. Sullivan and R. P. Woodbury, *J. Org. Chem.*, 1977, **42**, 3961-3963.
206 Y. Hashimoto and T. Mukaiyama, *Chem. Lett.*, 1986, 755-758.
207 Y. Hashimoto and T. Mukaiyama, *Chem. Lett.*, 1986, 1623-1626.
208 Z. Xie, L. Liu, W. Chen, H. Zheng, Q. Xu, H. Yuan and H. Lou, *Angew. Chem., Int. Ed.*, 2014, **53**, 3904-3908.
209 W. Chen, Z. Xie, H. Zheng, H. Lou and L. Liu, *Org. Lett.*, 2014, **16**, 5988-5991.
210 M. Wan, Z. Meng, H. Lou and L. Liu, *Angew. Chem., Int. Ed.*, 2014, **53**, 13845-13849.
211 Y. Wang, J. Zhu, R. Guo, H. Lindberg and Y.-M. Wang, *Chem. Sci.*, 2020, **11**, 12316-12322.
212 Y. Xia, N. W. Wade, P. N. Palermo, Y. Wang and Y.-M. Wang, *Chem. Commun.*, 2021, **57**, 13329-13332.
213 A. Yesilcimen, N.-C. Jiang, F. H. Gottlieb and M. Wasa, *J. Am. Chem. Soc.*, 2022, **144**, 6173-6179.
214 J. M. Allen and T. H. Lambert, *J. Am. Chem. Soc.*, 2011, **133**, 1260-1262.
215 W. Chen, L. Ma, A. Paul and D. Seidel, *Nat. Chem.*, 2018, **10**, 165-169.
216 C. F. de Grauw, J. A. Peters, H. van Bekkum and J. Huskens, *Synthesis*, 1994, 1007-1017.
217 G. Wittig and A. Hesse, *Liebigs Ann. Chem.*, 1971, **746**, 149-173.
218 J. Kim, A. Paul, I. Ghiviriga and D. Seidel, *Org. Lett.*, 2021, **23**, 797-801.
219 A. Paul, J. H. Kim, S. D. Daniel and D. Seidel, *Angew. Chem., Int. Ed.*, 2021, **60**, 1625-1628.
220 A. Paul and D. Seidel, *J. Am. Chem. Soc.*, 2019, **141**, 8778-8782.
221 W. Chen, A. Paul, K. A. Abboud and D. Seidel, *Nat. Chem.*, 2020, **12**, 545-550.
222 M. Shang, J. Z. Chan, M. Cao, Y. Chang, Q. Wang, B. Cook, S. Torker and M. Wasa, *J. Am. Chem. Soc.*, 2018, **140**, 10593-10601.
223 Y. Chang, M. Cao, J. Z. Chan, C. Zhao, Y. Wang, R. Yang and M. Wasa, *J. Am. Chem. Soc.*, 2021, **143**, 2441-2455.
224 Y. Chang, A. Yesilcimen, M. Cao, Y. Zhang, B. Zhang, J. Z. Chan and M. Wasa, *J. Am. Chem. Soc.*, 2019, **141**, 14570-14575.
225 J. Z. Chan, A. Yesilcimen, M. Cao, Y. Zhang, B. Zhang and M. Wasa, *J. Am. Chem. Soc.*, 2020, **142**, 16493-16505.
226 J. Z. Chan, Y. Chang and M. Wasa, *Org. Lett.*, 2019, **21**, 984-988.